

BEARING CAPACITY

OF PILES FROM

DYNAMIC MEASUREMENTS

FINAL REPORT

MARCH 1975

**PREPARED FOR: OHIO DEPARTMENT OF TRANSPORTATION
FEDERAL HIGHWAY ADMINISTRATION**

**DEPARTMENT OF CIVIL ENGINEERING
CASE WESTERN RESERVE UNIVERSITY
CLEVELAND, OHIO**

1. Report No. OHIO-DOT-05-75	2. Government Accession No.	3. Recipient's Catalog No.	
4. Title and Subtitle Bearing Capacity of Piles from Dynamic Measurements		5. Report Date March 1975	
		6. Performing Organization Code	
7. Author(s) G. G. Goble, Garland Likins, Jr., Frank Rausche		8. Performing Organization Report No.	
9. Performing Organization Name and Address Department of Solid Mechanics, Structures and Mechanical Design Case Western Reserve University Cleveland, Ohio 44106		10. Work Unit No. (TRAIS)	
		11. Contract or Grant No. State Job No. 14247(0)	
		13. Type of Report and Period Covered FINAL REPORT	
12. Sponsoring Agency Name and Address Ohio Department of Transportation Box 899 Columbus, Ohio 43216		14. Sponsoring Agency Code	
15. Supplementary Notes Study conducted in cooperation with the U. S. Department of Transportation, Federal Highway Administration			
16. Abstract A series of research projects have produced a reliable and accurate means of predicting static pile capacity from dynamic measurements. Instrumentation for measuring both force and acceleration at the pile top has been developed and tested. The signal is recorded on analog magnetic tape using a portable tape recorder. The necessary processing system, both hardware and software, has been assembled so that the recorded data can be analyzed completely automatically. The data is first converted to digital form and then a variety of computations are performed and the results plotted. A procedure, using the dynamic measurements, known as the Case Method has been studied which gives capacity predictions in excellent agreement with statically measured values. This method can be applied in the field using a special purpose computer. The concept was fully tested by the project. Methods were also developed for determination of resistance distribution along the pile using measurements made at the top. Extensive correlation between static measurements and dynamic predictions are presented for measurements made in Ohio and also in other states. In all 74 piles were tested.			
17. Key Words BRIDGE PIERS, DESIGN, DYNAMICS, FOUNDATIONS, IMPACT, PILE DRIVING, MEASURING INSTRUMENTS, SOIL MECHANICS		18. Distribution Statement	
19. Security Classif. (of this report) Unclassified	20. Security Classif. (of this page) Unclassified	21. No. of Pages 76	22. Price

F I N A L R E P O R T

BEARING CAPACITY OF PILES FROM DYNAMIC MEASUREMENTS

March 1975

by

G. G. Goble

Garland Likins, Jr.

Frank Rausche

Second Printing

This research was sponsored in cooperation with the Ohio Department of Transportation and the U. S. Department of Transportation, Federal Highway Administration. The opinions, findings and conclusions expressed in this publication are those of the authors and not necessarily those of the State or the Federal Highway Administration. This report does not constitute a standard, specification or regulation.

Case Western Reserve University
Department of Solid Mechanics, Structures and Mechanical Design
University Circle
Cleveland, Ohio 44106

ACKNOWLEDGMENTS

During the rather extended period which this project was active a large number of people, far too numerous to list, have made important contributions. Of particular importance is the assistance provided by many piling contractors in providing cooperation and free driving services. Some important contributors however should be mentioned. Without the advice and assistance of these people the project could never have reached a successful completion.

Ohio Department of Transportation

Bureau of Bridges
Raymond Grover

Bureau of Construction
Paul Eckhart
Richard Dowalter

Bureau of Research and Development
Ray Hanes
Leon Talbert

Case Western Reserve University
Prof. Fred Moses
Prof. Robert Scanlan

Graduate Students
John Tomko
W. S. LaPay
David Bubb
Kenneth Fricke

The Department of Transportation of
Idaho
Minnesota
Pennsylvania
New York
Georgia
Florida

The Prestressed Concrete Institute

The Foundation Equipment Company

PREFACE

This report is intended to serve a number of functions. First, it represents the final report on the most recent phase of the research project "Dynamic Studies on the Bearing Capacity of Piles". This phase was the fifth and last in a series which was sponsored at Case Western Reserve University by the Ohio Department of Transportation and the Federal Highway Administration. The new developments coming out of this phase of the work are reported here.

The second function of the report is to serve as a means for summarizing the results of a series of small projects sponsored by a number of state highway departments. These projects had as their goal the broadening of the data base.

The third and perhaps most important purpose of the report is to summarize the results of the total project and to present a state-of-the-art report on this approach to pile capacity determination.

PREFACE TO SECOND PRINTING

Additional data have frequently been requested by some readers. Therefore, further information on the test piles has been included in Table 2.1a, Page 45a.

TABLE OF CONTENTS

	<u>Page</u>
TECHNICAL REPORT STANDARD TITLE PAGE	i
UNIVERSITY TITLE PAGE	ii
ACKNOWLEDGMENTS	iii
PREFACE	iv
TABLE OF CONTENTS	v
CHAPTER I INTRODUCTION	1
CHAPTER II DATA ACQUISITION AND PROCESSING	3
2.1 Data Acquisition Equipment	3
2.2 Data Processing Equipment	6
2.3 Field Measurements	8
CHAPTER III CASE METHOD	12
3.1 Introduction	12
3.2 Wave Mechanics	13
3.3 Evaluation of Measurements	15
3.4 Time Delay Methods	19
3.5 Derivation of Damping Estimate	21
3.6 Results of Damping Approach	23
CHAPTER IV RESISTANCE DISTRIBUTION	28
4.1 Description of Resistance Distribution	28
4.2 Sample CAPWAP Results	30
CHAPTER V CONCLUSIONS	36
APPENDIX A	37
REFERENCES	38
TABLES	41
FIGURES	49

INTRODUCTION

The concept of using a Newton-based approach to the dynamic determination of pile capacity was first studied by Nara and Eiber (1)* at Case Institute of Technology. In 1964 the Ohio Department of Transportation began to sponsor research at Case to continue and expand this concept. The resulting series of research studies has already been extensively reported (2-11).

By 1970 it became apparent that the research results could be implemented for design and construction control of pile driving. However, there was a serious need for further data obtained on pile types and soils which had not been seen in Ohio. To meet this need, research sponsorship was sought from other state highway departments to provide data on piles which were being load tested statically to failure. The states of Idaho, Minnesota, Pennsylvania, New York, Georgia, and Florida responded to this request and piles were tested at a total of ten sites in these states. Pile types consisted of timber, prestressed concrete and steel pipes. Soil types ranged from clay to coarse sand. These projects have been reported previously (12-21) but summary results of these tests will be included in this report. Test work was also conducted in the state of Nevada under other arrangements with the Federal Highway Administration (the report on these tests is currently in progress) and the results are contained in this report.

In the past two years the authors have been called upon to perform consulting services for private agencies around the country. These tests have produced a substantial amount of data on piles which were statically load tested and these results are also contained in this report. Unfortunately, extensive soil data cannot be made available from these tests but the correlation between dynamic and static measurements is substantially expanded as a result of this data.

Project activities can be divided into four separate groups. First,

*Refers to references at end of text.

since the onset of the project there has been a continual development of instrumentation, data acquisition and data processing equipment. This work has continued through the current project and the current state of this equipment is described in Chapter 2. A second activity has been the continued development and refinement of the Case Method of capacity prediction (referred to as the "Simplified Method" in some previous reports). The Case Method capacity prediction involves simple computations and the most recent developments are described in Chapter 3. The third activity has been the development of the necessary analog electronic circuitry to make Case Method capacity predictions in the field. The resulting device appears to now be commercially viable. For the past two years development of this device has been carried on privately and has not caused the expenditure of project funds. However, as new field computers became available they have been used in project activities. The fourth activity has been the continued study and development of a computational technique known as the Case Pile Wave Analysis Program (CAPWAP). This computational procedure involves the determination of both static and dynamic resistances and their distribution in the pile using as inputs the measurements of force and acceleration made at the pile top. This requires a substantial amount of computational time on a large digital computer; therefore, the procedure cannot be performed in real time in the field. However, it does provide considerable potential for future application both in pile capacity prediction and in other types of activities. The CAPWAP computational procedure is discussed and some sample results are presented in Chapter 4.

The Case Method of pile capacity prediction has now progressed to the stage of routine application in pile design and construction control. At the present time (January, 1974) three state highway departments have acquired the Pile Capacity Analyzer and transducers to perform tests using their own personnel. In addition the Federal Highway Administration is involved in a demonstration project of this equipment and is currently using two Pile Capacity Analyzers in a demonstration project. Thus, it can be stated that implementation has been achieved and further expanded applications can be expected.

Chapter 2

Data Acquisition and Processing

2.1 Data Acquisition Equipment

The prediction of pile bearing capacity, computation of transferred energy and investigation of other dynamic quantities (i.e. maximum stresses, etc.) require the accurate measurement of force and acceleration at the pile top. In this Chapter the state-of-the-art for the routine measurement of these quantities will be described.

The acceleration measurements have become quite routine due to developments in electronics. Commercially available accelerometers are mounted on small aluminum blocks which are then bolted to the pile as shown in Figure 2.1. The mounting block must be as rigid as possible to avoid measuring accelerations arising from the response of the mounts. The total device must also be lightweight and mounted as close to the pile wall as possible to prevent large inertia forces due to the high accelerations in this mass. Piezoelectric accelerometers were used because of their high natural frequency and ruggedness. The particular model currently used is the PCB Piezotronics Model 302M21 with ground isolation. The model has a built-in amplifier to reduce problems of electronic noise from the cable. The nominal range is 1000 g's with a maximum shock limit of 5000 g's. The nominal sensitivity is 5 millivolts/g. This accelerometer has a frequency range of 1 to 5000 Hz with a resonant frequency greater than 30,000 Hz. Results have been satisfactory.

The measurement of force has had more project involvement. Initially the force was measured by attaching resistance strain gages directly to the steel pile wall. The strain was converted to force using the known material modulus and cross sectional area of the steel pile. Routine application of this technique for a large number of piles under all weather conditions is not a reasonable procedure. Reusable transducers are desirable in that they reduce the time required for attachment and number of the strain gages used. Thus, the total cost and time lost to the contractor for making a routine test is reduced. These transducers

are constructed and calibrated in the laboratory.

Two types of transducers were developed. One type introduces a force measuring device between the pile and the hammer. The force transducer is relatively lightweight compared with that used in other studies (22) and thus avoids most of the difficulty experienced. Results from this transducer have been compared with strain gages mounted directly on the pile with very good agreement. This transducer attempts to match the cross section shape of the actual pile with a small increase in wall thickness. If damage occurs near the pile top, the transducer's increased wall thickness forces the damage to be in the pile, therefore preventing costly damage to the transducer itself. For the common 12-inch pipe piles used in Ohio with a wall thickness of 0.179 inches, a 12-inch diameter pipe with a 3/8 inch wall thickness and 12-inch length has performed satisfactorily. A force transducer is shown in Figure 2.2. At the mid-length of this pipe six dual element resistance strain gages are attached at 60 degree intervals to minimize local bending and end effects and obtain the average force in the pipe. One element is parallel and the other transverse to the axis of the pipe. All gages have 120 ohms resistance and are wired three elements in series in each leg of a full bridge. One inch thick, 14-inch steel plates were welded to the top and bottom of this pipe. An 11-inch diameter hole was cut in these plates to minimize the transducer weight and the introduction of bending effects at the ends. The upper end of the transducer is bolted to another section of 12-inch pipe welded on one end to another heavy plate. This top adapter then accepts the driving helmet in exactly the same manner as would the actual pile. The bottom adapter is an undersized pipe which is welded to another heavy plate which is then bolted to the transducer. The bottom adapter then becomes a male adapter having a snug fit inside the pile top. High frequency accelerations can be mechanically filtered out by introducing plywood cushions between the transducer and top adapter. The use of more than two inches of plywood is discouraged as it modifies the actual event by an amount undesirable for use with the Case Method.

The linearity of this transducer is excellent and hysteresis is not

noticeable during static calibration in a 200 kip universal testing machine. Transducers of this type have also been constructed for 14-inch and 10-inch pipes with equally satisfactory results. Transducers for steel H piles have been constructed with somewhat less satisfactory results. Due to the less regular shape it appears that the transducer length must be increased or the number of strain gages increased to avoid serious problems of linearity. The bottom adapter is also not as simple. Some type of fitting must be made to guide the transducer to fit well over the pile top or the heavy plate to which the transducer bolts must be tack welded directly to the pile top for each pile tested.

Force transducers for concrete and timber piles have not been satisfactorily designed.

The second type of force measuring device can more accurately be described as a strain transducer. The current design is shown in Figure 2.1. This diamond shaped frame is attached to the pile at two points three inches apart along the pile axis. Four 350 ohm strain gages are attached to the "hinge" locations and are again wired in a full bridge arrangement. This frame then measures the average strain between the two points. If the strain transducer is too stiff, large forces are transmitted to the attachment points which can cause yielding of the transducer or slippage with respect to the pile causing apparent large residual forces in the pile. The current design is very flexible (an axial static test of the transducer alone caused 3000 $\mu\epsilon$ from only six pounds). To avoid undesirable effects of inertia forces it is also lightweight and attached close to the pile wall.

Because of their weight and size, the strain transducers are easily transported to different job sites. They can be attached to any pile type, shape or size. Clearance holes for 1/4 - 20 bolts are drilled in thin wall steel sections and the transducers mounted with bolts and nuts. In thick wall steel sections the holes can be drilled and tapped. Concrete piles are instrumented by drilling a 1/2-inch diameter, 1 inch deep hole and setting anchors for the 1/4 - 20 bolts. A 1/8-inch pilot hole is drilled in timber piles and the transducer is

then attached with lag bolts. The recorded strain is then converted to force using the pile area and material modulus. For steel piles these values are well known. However, for concrete and timber piles the dynamic modulus must be computed from the wave speed, c , by

$$E = \rho c^2 \quad (2.1)$$

where ρ is the mass density. The density of concrete can be assumed to be 150 pounds per cubic foot. The density of creosoted timber varies widely from 40 to 70 lb/ft³ and, if an accurate modulus is to be determined, must be measured. The wave speed determination is a simple process and has been described elsewhere (13, 16, 17).

To cancel any bending effects in the pile, two accelerometers and two strain transducers are attached diametrically opposite as shown in Figures 2.1 and 2.3. The cables from each transducer are connected to a connection box as in Figure 2.3. A single connection cable carrying all signals then goes to a power supply for the accelerometers and a signal conditioning and balancing unit for the strain. The output can then be observed on an oscilloscope or recorded on a high speed oscillograph or analog FM tape recorder for later analysis. The tape recorder gives the advantage of being able to recreate the electronic signal recorded. Thus, processing can be more efficient and accurate.

2.2 Data Processing Equipment

Upon returning from the field, the analog magnetic tape data are analyzed using the Case Project processing system. The data are automatically converted to digital form using an analog-to-digital converter controlled by a small digital computer. Those portions of the record containing the hammer blow are then stored on digital magnetic tape for further analysis. The acceleration record is integrated to obtain displacement. The final displacement can be compared with the driving record and if necessary the acceleration zero can be adjusted to give the correct final set. It should be emphasized that all of the above processing steps are performed automatically. It is

important that as many checks as possible be performed on the data to assure its correctness. For instance, it is known that force and velocity are proportional at impact. Since these two quantities are obtained by two quite different measurement systems their comparison represents a particularly effective check.

The records of force and velocity are then used to predict the pile's static capacity. If the data was taken at the end of driving, the Case Method capacity gives the static capacity at this time. The last blows are the most important. If data was taken during a restrike, the service conditions of the pile including any set-up or relaxation effects are given. During restrike, the loss of these time dependent effects can occur and, therefore, the first blows are the most critical.

Maximum pile top accelerations, velocities, displacements, forces, stresses, and Case Method capacities are also printed for each blow analyzed. Hammer energy transferred to the pile can be calculated from the expression

$$E(t') = \int_0^{t'} F(t) v(t) dt \quad (2.2)$$

where the energy, $E(t)$, force, $F(t)$, and velocity, $v(t)$, are all functions of time. This is the energy available to the pile to do work and it eliminates the uncertainty regarding the magnitude of impact losses due to heat, friction, sound, combustion efficiencies or ram impact velocity, and in elastic collisions in the drive cap assembly. The maximum and final energies (after pile rebound occurs) are also printed. In addition, plots of acceleration, velocity, displacement, force and energy may be plotted on a CALCOMP drum plotter as functions of time. An example of these plots is shown in Figure 2.4.

Sample blows are then punched on punch paper tape and transferred to a large digital computer for wave equation analysis.

2.3 Field Measurements

Since the ultimate goal of this project has been to develop an easy-to-use method of accurately predicting a pile's static bearing capacity, the dynamic testing of piles which were also statically tested was emphasized. Only in this way could the techniques and prediction reliability be tested and improved.

As early as December 1964 project personnel were given the opportunity to make dynamic measurements on piles which were also statically tested by the Ohio Department of Transportation. Data at that time was taken by strain gages mounted directly on the pile wall and recorded on a high speed oscillograph. During the next few years transducer development produced the reuseable force and strain transducers which were checked for accuracy by comparison of the record with strain gages mounted on the same pile. Accelerometers which were more rugged and had less electronic noise were also obtained. Through 1970 because of the limitations of the oscillograph, only a few blows per pile were recorded. They had to be manually converted to digital form for further analysis. The results from several of these early piles have since been determined to be of questionable accuracy. Many of the piles seem to have errors in their calibration of force or acceleration which are irretrievable. In some cases the oscillograph records were not converted to digital form with sufficient accuracy. For these reasons these piles are no longer being used for correlation with capacity.

During the summer of 1970 the portable tape recorder became available due to a special grant from the Prestressed Concrete Institute and it was then used to record the data. In replacing the oscillograph, calibration errors were virtually eliminated and digital conversion, controlled by a small computer, made it possible to analyze a large volume of data faster and with greater accuracy. This made pile testing more accurate and routine. As the reliability of the results improved more opportunities became available to make the field measurements and compare predicted and measured capacity. This also provided ample opportunity to further improve

the transducers. During this time analog computer for field determination of static capacity had reached the stage where it could be routinely used as the pile was being driven. Results were good and the computer has since been further modified and improved and is now in routine use by several organizations. On many jobs this testing procedure has replaced or reduced static testing with large cost savings. Use of the technique has also been applied to the quality control of production piling to insure uniformity over the job site by random testing. Additionally, since results are obtained for every blow, capacity as a function of penetration can be easily investigated to reveal the most suitable bearing stratum and make more efficient use of static load tests.

The current list of piles where static and dynamic test results are available is given in Table 2.1. This data set provides the basis for correlation of Case Method capacity prediction with actual static load tests run to failure. Piles where load tests were not run to failure or where no static test was made are not reported in this list. The majority of the piles tested for the Ohio Department of Transportation were 12 inch cast-in-place closed-end steel pipes. In Ohio these piles are typically 40 to 80 feet in length.

Cooperative projects were also begun in 1971 with various other state highway departments to expand the measurements to pile types which are not commonly used in Ohio. As a result of this activity, fourteen statically load tested piles were added to the data base, and the capability and reliability to test timber and prestressed concrete piles was proven. Also at about the same time a demand appeared from private agencies for this service on a consulting basis. The result has again been an increase of dynamically measured static load test piles. These 19 piles have been included in Table 2.1 as Consulting Piles (CP1, CP2, ..., CP19) and are numbered in chronological order.

The 74 piles reported here are of several types. A total of 46 of the piles were either closed end cast-in-place (CIP) steel pipe piles or mono-tube. In fact, the first 27 load tested piles measured by project personnel were of this type since they represent the standard Ohio Department of

Transportation pile where it is not driven to rock. Ten of the piles were timber piles and only three were steel H-pile sections. The remaining 15 piles were prestressed concrete piles of various cross section. The most common sections were solid, ranging from 10 to 18 inches square. Two of these piles were solid octagonal sections with a 14 inch "diameter".

The hammers used to test the piles were of several types; 5 were double acting air steam hammers, 9 were single acting air steam, 20 were double acting diesel, and 40 were single acting diesel. These were the hammers being used on the job sites and were not selected for any other reasons. In general the diesel hammers are those which are most commonly seen in the midwest. The air steam hammers were used in states which have restrictions on hammer types. No noticeable difference in the reliability of the Case Method capacity prediction has been observed for any hammer type.

The pile lengths have varied from about 25 feet to 140 feet for the load test piles reported here. Longer piles have been tested but were not statically loaded or had no soil boring available. Shorter piles have been tested but it should be noted that the time required for the force increase at impact becomes longer when compared to the time required for the Case Method. Conceivably this can adversely affect the prediction reliability and for this reason short piles have been discouraged.

Also included in Table 2.1 is a general soil description for the piles. The soil at the pile tip is most important for the Case Method capacity predictions. The prevailing soil type along the pile is also given in cases where the side soil is greatly different from that at the pile tip. A wide variety of soil types can be observed.

In addition to the load tested piles reported here, measurements of many additional piles have been made. On most construction sites where static tests were performed, in addition to the test pile several other job piles were randomly tested to insure uniformity over the job site. It is not uncommon to test three to five additional piles in this manner.

As the reliability of the method has improved it has become increasingly common that dynamic measurements have completely replaced static testing on many sites. As a result several hundred dynamically measured piles have also been tested in addition to the 74 piles in Table 2.1.

Chapter 3

Case Method

3.1 Introduction

The Case Method of pile capacity determination has been used with increasing frequency during the past two years for both design and construction control of impact driven piles. As an increasing amount of static load test data became available for correlation the computation methods were modified, improved and refined.

The previous derivation of the fundamental Case Method equation has generally been preceded by the assumption that the pile be treated as a rigid body. The expression resulting from the application of Newton's Second Law has then been modified without a complete derivation being presented with only a general reference to wave equation analysis. This type of presentation has caused the method to be criticized unjustly as being based on a rigid body assumption. The relationship was first derived and presented in Reference 4. It will be developed here in a brief way that will, perhaps, be more readable. Also the various modifications which are necessary to account for different soil and pile types are discussed.

In order to illustrate many of the characteristics of pile mechanics a typical force and velocity record for an impact driven pile is shown in Figure 3.1, where the velocity was obtained by integrating the measured acceleration over time. Also, for ease of plotting the velocity was multiplied by a constant, EA/c (Young's modulus times cross sectional area divided by the wave speed; all pile quantities). The time scale is given in milliseconds and in L/c units, i.e. in units of that time which a stress wave needs to travel along a pile of length L .

This record was obtained from a 25 ft. long concrete pile driven by a Delmag D-30 Diesel hammer. The static resistance as determined by a load test was 550 kips which is low compared to the force at impact. As a result the pile top force decreases at time $2L/c$ after impact, i.e.

when the impact wave returns after a (tension) reflection at the pile bottom.

3.2 Wave Mechanics

In the subsequent discussion it is assumed that the bar or pile is of uniform cross section. The derivation and solution of the one dimensional wave equation, a linear, second order differential equation, is available from other sources (23) and will not be presented here.

Figure 3.1 shows one important phenomenon of wave mechanics, namely the fact that force and velocity at a point on a bar are proportional as long as stress waves at this point travel in only one direction. A wave in a rod which is free at top and bottom always has the same direction of velocity (while the sign of stress changes upon each reflection). The proportionality between the two curves is destroyed as soon as waves caused by soil resistance forces reach the pile top. However, for a completely free pile the top velocity due to a pile top force, $F_t(t)$, can be written

$$v_{t,F}(t) = \frac{c}{EA} F_t(t) \quad 3.1$$

for $0 \leq t < \frac{2L}{c}$

At times later than $2L/c$ the effect of waves reflected from the pile bottom is felt at the top. Since a free top is assumed, the velocity will be doubled under reflection and will always be positive (4).

Therefore

$$v_{t,F}(t) = \frac{2c}{EA} \left\{ \frac{1}{2} F_t(t) + F_t\left(t - \frac{2L}{c}\right) + F_t\left(t - \frac{4L}{c}\right) + \dots \right\} \quad 3.2$$

Resistance forces create a somewhat more complex wave behavior in a pile, since they, in general, act at intermediate locations along the pile. A suddenly applied force at such an intermediate location produces

two waves. If the force, as in the case of soil resistance at a location x , $R_x(t)$, is directed upwards then the upwards traveling wave will be in compression and the downwards traveling one in tension. For reasons of continuity and equilibrium, together with the proportionality requirement between force and velocity, the forces in each wave must have a magnitude that is one half of the applied force. The velocities in both waves at the point of force application, x_i , are:

$$v_{t,Fi}(t) = \frac{1}{2} \frac{c}{EA} R_{x_i}(t) \quad 3.3$$

Dealing again with a free pile on which this resistance force acts, the velocities will always be directed upwards. The pile top velocity when either of the two waves arrives and reflects will be twice the magnitude of that in Equation 3.3. The only difference between the two waves is in the arrival time. The upwards traveling wave arrives earlier than the other wave which is first reflected from the bottom.

Assuming that the distributed soil resistance is concentrated at n locations, x_i , $i = 1, \dots, n$ (x_i measured from the top) whose magnitudes are R_i , $i = 1, \dots, n$ and which are of the ideal plastic type such that

$$R_{x_i}(t) = R_i H\left(t - \frac{x_i}{c}\right) \quad 3.4$$

where $H(t - a)$ is the Heavyside step function which is 0 for $t < a$ (negative arguments) and 1 for $t \geq a$. With $t = 0$ being the time of impact this soil resistance law implies that the resistance forces act only after the impact wave has reached their respective location and that they are constant thereafter.

The effect of the upwards traveling wave caused by $R_{x_i}(t)$ is felt at the top with a time delay x_i/c , and that of the downwards traveling wave with a delay $(2L - x_i)/c$ (after reflection at the bottom). This means that the first effect of $R_{x_i}(t)$ carried by the downwards traveling

wave is felt together with the bottom reflected impact wave at time $2L/c$ after impact.

For all times one can write the top velocity due to the upwards traveling velocity caused by $R_{x_i}(t)$ as

$$v_{t,i}^u(t) = -\frac{c}{EA} R_i \left\{ H\left(t - \frac{2x_i}{c}\right) + H\left(t - \frac{2x_i + 2L}{c}\right) + H\left(t - \frac{2x_i + 4L}{c}\right) + \dots \right\} \quad 3.5$$

remembering again that because of the reflection at the free top the wave velocity has doubled.

The downwards traveling wave causes a top velocity

$$v_{t,i}^d(t) = -\frac{c}{EA} R_i \left\{ H\left(t - \frac{2L}{c}\right) + H\left(t - \frac{4L}{c}\right) + H\left(t - \frac{6L}{c}\right) + \dots \right\} \quad 3.6$$

The total velocity caused by the impact force, $F_t(t)$, and all n resistance forces R_i , $i = 1, 2, \dots, n$ can be written as

$$v_t(t) = \frac{c}{EA} \left\{ F_t(t) + 2 \sum_{j=1}^m F_t\left(t - \frac{j2L}{c}\right) - \sum_{i=1}^n R_i \left[H\left(t - \frac{2x_i}{c}\right) + \sum_{j=1}^m H\left(t - \frac{2x_i + j2L}{c}\right) + \sum_{j=1}^m H\left(t - \frac{j2L}{c}\right) \right] \right\} \quad 3.7$$

where m indicates the time interval after impact:

$$\frac{m2L}{c} < t < \frac{(m+1)2L}{c}$$

3.3 Evaluation of Measurements

If this simplified soil model for the resistance force were correct then $v_t(t)$ would be equal to $v_M(t)$ (i.e. the measured velocity) when the measured force $F_M(t)$ was substituted for $F_t(t)$ in Equation 3.7. Thus,

$$\frac{EA}{c} v_M(t) = F_M(t) + 2 \sum_{j=1}^m F_M(t - \frac{j2L}{c})$$

$$- \sum_{i=1}^n R_i \left[H(t - \frac{2x_i}{c}) + \sum_{j=1}^m H(t - \frac{2x_i + j2L}{c}) + \sum_{j=1}^m H(t - \frac{j2L}{c}) \right] \quad 3.8$$

The third term in Equation 3.8, the summation over all resistance forces is shown graphically in Figure 3.2. The first portion of the term is due to the first arrival at the pile top of the upward traveling wave due to the resistance at the location x_i . The full value is felt at $\frac{2x_i}{c}$ after impact and stays on for the remainder of the blow as shown by the solid bar in Figure 3.2. The second portion of the term is due to the same wave after reflections from the top and bottom. Thus, for the first and succeeding time intervals m the effects are felt $2L/c$ after the preceding interval $m-1$, and are represented by the striped bars in Figure 3.2. The third portion of the third term is due to the effect of the downward traveling wave. The wave arrives at $2L/c$ after impact and again remains on for the remainder of the blow. Due to subsequent reflections the same effect is felt every $2L/c$. This portion is depicted by the white bars in Figure 3.2. Since all of these effects are of equal magnitude it can be seen from Figure 3.2 that the third term becomes

$$- \sum_{i=1}^n R_i \left[2m + H(t - \frac{2x_i + 2mL}{c}) \right] \quad 3.9$$

where m is the time interval. If the measured velocity is taken at any time t^*

$$(m \frac{2L}{c} \leq t^* < (m+1) \frac{2L}{c})$$

and if the measured velocity at a time $2L/c$ later is subtracted, then the result is

$$\begin{aligned}
\frac{EA}{c} \{v_M(t^*) - v_M(t^* + \frac{2L}{c})\} &= F_M(t^*) + 2 \sum_{j=1}^m F_M(t^* - \frac{j2L}{c}) \\
&\quad - F(t^* + \frac{2L}{c}) - 2 \sum_{j=1}^{m+1} F_M(t^* + \frac{2L}{c} - \frac{j2L}{c}) \\
&\quad - \sum_{i=1}^n R_i [2m + H(t^* - \frac{2x_i + 2mL}{c}) - 2(m+1) \\
&\quad \quad - H(t^* + \frac{2L}{c} - \frac{2x_i + 2(m+1)L}{c})] \tag{3.10}
\end{aligned}$$

Since the arguments of the Heavyside function terms both have the same value their effects cancel. In addition the first element of the fourth term becomes

$$-2 F_M(t^* + \frac{2L}{c} - \frac{2L}{c})$$

and combines with $F_M(t^*)$ to produce $-F_M(t^*)$. The simplified expression then becomes

$$\frac{EA}{c} \{(v_M(t^*) - v_M(t^* + \frac{2L}{c}))\} = -F_M(t^*) - F_M(t^* + \frac{2L}{c}) - \sum_{i=1}^n R_i \{2m - 2(m+1)\} \tag{3.11}$$

and with:

$$\sum_{i=1}^n R_i = R \tag{3.12}$$

i.e. the total resistance, yields

$$R = \frac{1}{2} \{(F_M(t^*) + F_M(t^* + \frac{2L}{c})) + \frac{EA}{c} (v_M(t^*) - v_M(t^* + \frac{2L}{c}))\} \tag{3.13}$$

For a uniform rod with

$$c = \sqrt{E/\rho} \quad 3.14$$

and $M = LA\rho$ (ρ is the mass density, M the total pile mass) direct substitution gives

$$\frac{EA}{c} = \frac{Mc}{L} \quad 3.15$$

Thus, Equation 3.13 can also be written as

$$R = \frac{1}{2} \left\{ F_M(t^*) + F_M\left(t^* + \frac{2L}{c}\right) \right\} + M \frac{v_M(t^*) + v_M\left(t^* + \frac{2L}{c}\right)}{2L/c} \quad 3.13a$$

which shows that the prediction R can be considered as an average of two force values $2L/c$ apart plus an inertia term using an average acceleration over the same time period. Equation 3.13a reduces to Newton's Second Law as L approaches zero.

While the pile elastic properties and the distribution of resistance forces were properly considered in the above derivation, the resistance force versus time variations were neglected. These variations exist because both dynamic resistance forces (soil damping) and unloading (pile rebound) occur.

Originally (2) it was proposed to choose the time t^* , yet to be decided upon, at the time when the pile top velocity became zero. Then, it was argued, soil damping forces would have become small. Results obtained in this way were usually somewhat low when compared with the ultimate capacity of the pile as determined in a static load test. There was an indication, however, that a correct correlation was to be made with a penetration related capacity (less than ultimate). This approach has been abandoned as it is difficult to use in construction control

Later, it was found, when analyzing data from piles whose capacity was large compared to the hammer driving capability, or which had long lengths L ($t^* + 2L/c$ was then at a very late time) that unloading had occurred. The predictions were then too low.

For steel pipe piles in granular soils empirical correlation with ultimate capacity was best when choosing t^* at the time when the first relative maximum of velocity was reached (here called the time of impact). Such empirical correlation studies showed, further, that piles in cohesive soils required some time delay between the time of impact and t^* .

3.4 Time Delay Methods

The Case Method capacity equation is

$$R = \frac{F(t^*) + F(t^* + \frac{2L}{c})}{2} + \frac{Mc}{2L} [v(t^*) - v(t^* + \frac{2L}{c})] \quad 3.16$$

This procedure using dynamic measurements has been applied to 60 piles which were also statically load tested. A wide variety of pile types, soil conditions, and hammer combinations are now represented and the results are very promising. Depending upon the pile-soil combination, dynamic forces, commonly called damping, related to the relative pile velocity can occur. For most pile types the majority of both the static soil resistance and dynamic forces have their origin at the pile tip rather than in frictional side resistance. This hypothesis has been confirmed by using a wave equation analysis on the dynamically measured data (4) and also through strain gages located along the pile length where readings were taken during the static load tests. Because the largest static resistances usually occur at the pile toe an extensive study was performed to correlate the time t^* with the pile type and soil type at the pile toe. If the time t^* is chosen as the time of the first velocity maximum, t_{\max} , the Case Method capacity, given by Equation 3.16 is a good approximation to the sum of static resistance and the maximum damping. If damping forces are negligible, then using

t_{\max} for t^* in the Case Method should yield a good estimate of the static capacity. For pipe piles driven into a sand, the use of the wave equation on dynamically measured force and acceleration showed very little damping. In this situation the Case Method using t_{\max} has done very well in predicting the static capacity.

In cases where pipe piles have been driven into a finer grained bearing stratum such as silt or clay, damping forces can be substantial (to the point of exceeding the static resistance) and using t_{\max} could lead to errors in Case Method. Between t_{\max} and $2L/c$ later the velocities in the pile are usually at their largest magnitude. Since damping forces are proportional to pile velocity, it is logical that to reduce damping forces it is necessary to wait until the velocities in the pile are smaller. A time delay from the time of the first relative maximum in velocity, t_{\max} , then becomes necessary. Because time, referenced to the pile, is measured in $2L/c$ units the expression for t^* in the Case Method Equation 3.16 becomes

$$t^* = t_{\max} + \delta \left(\frac{2L}{c} \right) \quad 3.17$$

The computational procedure is illustrated on a sample measurement record in Figure 3.3.

For pipe piles various constants, δ , were tried for various soil conditions. Results can be seen in Figure 3.4. The solid bars represent those regions of δ -values which give a Case Method prediction within 15% of the load test value. For nonplastic silt δ is chosen as 0.25; for weak plastic silt and soft clay δ is 1.40; for stiff clay δ is chosen as 1.20. It would appear that as the soil bearing stratum becomes weaker (as determined from the soil boring logs) the delay time must be increased. For pile types other than steel pipe piles, similar analyses of the data were made.

As the pile weight and stiffness of timber piles is similar to that of steel pipe piles, the δ -values for the various soil conditions for pipe piles apply equally well to timber piles. For concrete piles the

large pile mass can cause large predictions due to the acceleration related inertia term in Equation 3.16. Large forces also occur at impact. If the bearing stratum is strong, no time delay is necessary; however, δ -values of 0.25 have been used successfully on all concrete piles. For prestressed concrete piles in weaker material, larger δ -values also work well. More data is needed. For H piles not driven to rock the static resistance gained purely from point bearing is smaller than for other pile types driven in a similar soil. Pile tip damping is also increased. From the limited data acquired on H piles to date a δ -value of 1.50 seems appropriate.

Results of all Case Method predictions for all pile soil types using the values recommended above are plotted against the corresponding static load test in Figure 3.5. Using a least squares correlation routine, a correlation coefficient of 0.981 was obtained with a standard deviation of 19.7 kips. The average predicted divided by measured value was 1.01. Differences due to the definition of failure for a static test are as large as the scatter represented here. The results for various pile types are shown separately in Figures 3.6-3.9.

3.5 Derivation of Damping Estimate

Equation 3.13a has been derived using a very simple model for soil behavior. An improvement in this model and a commonly used approximation is to assume that the forces R_i are really made up of two portions. The first portion is due to static resistance forces $R_{i,s}$ and their sum R_s is then the actual failure load. The second portion $R_{i,d}$ is due to dynamic resistance forces (damping) which are usually treated as being proportional to velocity. The sum of these dynamic forces R_D is important only during the driving of the pile and is of no further practical value. Thus, the total driving resistance R can be broken up into two distinct portions

$$R = R_S + R_D \quad 3.18$$

In order to more closely approximate the pile's static capacity from dynamic measurements an estimate of the total damping forces R_D must be made.

Because the damping effects of soil and unloading due to pile rebound diminish the force and velocity waves in a rather short time period, only the first $2L/c$ period is usually available for estimation of the maximum damping resistance R_D . Further, as described in Section 3.6 the majority of this damping resistance is concentrated near the pile tip. The bottom velocity of the pile for the free pile solution after the impact velocity arrives and reflects is

$$v_B(t) = 2 v_t(t - \frac{L}{c}) \quad 3.19$$

for $\frac{L}{c} \leq t \leq \frac{3L}{c}$.

The effect of the downwards traveling wave caused by $R_{x_i}(t)$ on the bottom velocity is given by twice the magnitude of Equation 3.3 due to reflection.

$$v_{B,i}^d(t) = -\frac{c}{EA} R_i H(t - \frac{L - x_i}{c}) = -\frac{c}{EA} R_i \quad 3.20$$

for $\frac{L}{c} \leq t \leq \frac{3L}{c}$.

The pile top velocity characteristically shows a relative maximum in the beginning of the blow (impact) and then diminishes in magnitude with time. In cases of very easy driving, the large tip penetrations and tensile reflections cause a large increase in pile velocity at $2L/c$ after impact. In several cases the top velocity after the impact reflection from the weak tip can become significantly larger than the pile velocity at impact. Because piles are rarely considered acceptable for capacity in such easy driving, they are not of great importance. However, in the cases where they have been encountered by the project the velocity estimates are satisfactory. The bottom velocity will reach a relative maximum value at time $t = t_{\max} + \frac{L}{c}$ (t_{\max} is the time of impact) and is given by

$$v_{B,\max}(t_{\max} + \frac{L}{c}) = 2v(t_{\max}) - \frac{c}{EA} \sum_{i=1}^n R_i \quad 3.21$$

(The effect of the upward traveling wave caused by R_{x_i} will be zero at time L/c because all Heavyside step functions $H(t - \frac{L + 2x_i}{c})$ are zero).

If the damping force is treated as proportional to this bottom velocity then the maximum damping force becomes

$$R_{D,max} = b v_{B,max} = J_c \frac{EA}{c} v_{B,max} \quad 3.22$$

where J_c is a dimensionless damping parameter (see Appendix A). Use of Equation 3.13a with t^* equal to t_{max} gives the maximum driving resistance R_{max} . Rearranging Equation 3.18 and using Equations 3.1, 3.12, 3.21 and 3.22 gives the maximum static resistance $R_{S,max}$ as

$$R_{S,max} = R_{max} - J_c \left(2 \frac{EA}{c} v_t(t_{max}) - R_{max} \right) \quad 3.23a$$

or

$$R_{S,max} = R_{max} - J_c \left(2 F_t(t_{max}) - R_{max} \right) \quad 3.23b$$

Use of Equation 3.23 can then be made with the measured force and velocity functions of time and the actual failure load of the pile as determined from a static load test to determine the correct value of J_c for any particular pile.

3.6 Results of Damping Approach

For most piles, if the damping can be assumed to be concentrated at the pile tip, the actual damping resistance was shown in Equation 3.23 to be proportional to the pile properties (EA/c), bottom velocity (which can be calculated from the top velocity, pile properties and total driving resistance), and a damping constant J_c which is related to the soil type at the pile tip. Data has been obtained on 71 test piles where static load test capacity, sufficient soil borings, and total

driving resistance R_{\max} are available. This approach was investigated several months after the time delay methods. During the intervening period eleven additional static test piles were tested which bring the total data set to 71 piles. Of these piles, 43 are closed end steel pipes, 15 are prestressed concrete, ten are timber and three are H piles. For each pile a damping constant J_c was calculated which produced a prediction which was equal to the static load test value. In addition damping constants which produce only 20 percent error in Case Method prediction were determined. Any damping constant J_c chosen between these two limiting values will give a Case Method prediction which will be in error from the static load test value by less than 20 percent. Negative damping constants are physically meaningless and are therefore set to zero should they occur. A plot of the non-negative damping constant J_c within 20 percent of the load test value is given as a function of soil type regardless of pile type (because all pile types show the same characteristics) in Figure 3.10. For piles with an ultimate capacity less than 150 kips the 20 percent range becomes less than 30 kips. Measurement errors in the dynamic and static tests as well as the type and interpretation of the static load test failure appear to dictate for these low capacity piles that an error range of 30 kips instead of 20 percent be considered acceptable. This additional range in the acceptable damping constant value is indicated in Figure 3.10 with the dashed lines. It can be seen that as the soil grains become finer the damping constant, J_c , must become larger. This was the expected result.

For any given soil type on any job site where a static test is also run, a dynamic test on the static test pile will give the correct damping constant which can then be used on all remaining dynamically tested piles driven to the same soil stratum. For job sites with no static test to correlate with, the previous experiences shown in Figure 3.10 can then serve as a guide in choosing the proper damping constant which will yield a Case Method prediction within 20 percent of the static test result with a good degree of confidence. Recommended values are J_c equal to 0.05 for sand, 0.15 for silty sand, 0.2 for sandy

silt, 0.3 for silt, 0.55 for silty clays and clayey silt, and 1.1 for clay. The seemingly high value for clay is to protect against a possible failure in a soil type where relatively little experience has thus far been obtained. It should be noted from Equation 3.23 that as the damping constant is increased the resulting static prediction becomes more conservative. Thus, to assure that the Case Method is conservative, a higher damping constant than would normally be associated with the soil type need only be selected. It can be seen that the above recommended values are within 20 percent or are at least conservative in all but three cases. Two of these cases were for very low capacity piles in silty clay which were not production piling, but rather were driven especially for project personnel in the early stages of the project when measurement techniques were not as advanced. The third pile was within 25 percent. In general, the results of the Case Method using damping proportional the pile cross section properties EA/c appear very promising. A plot of the predicted versus measured capacities using the Case damping applied to the Case Method prediction is shown in Figure 3.11, and uses the above recommended damping constants.

One additional damping approach was considered. In the approach originally developed by Smith for the wave equation, the damping was assumed to be proportional to the static soil resistance (24). The expression for the damping then becomes

$$R_{D_s} = J_s R_s v_{\text{bottom}} \quad 3.24$$

and the expression for the static resistance after rearranging then becomes

$$R_s = \frac{R_{\text{max}}}{(1 + J_s v_{\text{bottom}})} \quad 3.25$$

The same 20 percent or 30 kip (whichever is greater) criteria was applied to the pile with this equation. The results are shown in Figure 3.12 with the damping constant J_s as a function of soil type. The differences

between the two definitions of damping cause rather large differences. The magnitude of the Smith damping constants J_s are only about one tenth those of the Case damping constants J_c . Piles with low capacity seem to exhibit higher damping constants than do the higher capacity piles in the same soil type. It is possible that this is due to the definition of failure in the static tests (a constant error is a larger percentage in the low capacity piles). Due to the division of the damping term in the Smith method, as opposed to the linear subtraction of the Case damping, the low capacity piles have comparatively large ranges of acceptable Smith damping constants. In addition the Smith prediction cannot go negative but will only asymptotically approach zero as the product $J_s V_{\text{bottom}}$ becomes large. One last point is that when the pile capacity is small, the pile capacity R_s is more closely equal to the pile property EA/c and the damping constant more closely approaches the more natural Case damping approach. The combination of the above factors makes the Smith damping approach a good one for low capacity piles if the damping constant J_s is chosen slightly higher than higher capacity piles in the same soil type.

For piles where the static capacity R_s is close to the ultimate driving resistance R_{max} , the damping constant J_s must be small and carefully selected or else large errors can result due to the division. For piles with normal or high capacity the following Smith damping constants are recommended based on current experience: J_s equals 0.010 for sand, 0.015 for silty sand and 0.020 for sandy silt, 0.035 for silt, 0.040 for clayey silt and silty clay, and 0.090 for clays. The user must be aware that these values will give very unconservative results for low capacity piles as shown in Figure 3.12. The above recommended values give results which are within the 20 percent (or 30 kips) or are conservative in all but six cases. Four of these cases are low capacity piles which have already been noted as giving unsatisfactory results unless the coefficient is increased. The other two piles which are undesirably non-conservative were concrete piles in clay and in sandy silt and were in error by 50.8 and 28.3 percent respectively. To be in error by 50 percent unconservatively is to

eliminate the common factor of safety of 2.0 completely. This is very undesirable. Because of such features it is advisable to also compute the capacity using the Case damping approach and if the numbers are greatly different then use the lower of the two capacity estimates. It is often impossible to judge a priori whether or not the pile is a low capacity pile and that the Smith damping constant should be increased. In addition there is no rational reason that the dynamic resistance is directly proportional to the static capacity. For these reasons it would appear that the Case damping approach (damping proportional to pile properties and not static capacity) is the better method.

In addition to the piles reported here, three closed end steel pipes had computed bottom velocities which were negative. As this was physically meaningless the damping was assumed to be zero. The resulting error from using the entire maximum driving resistance R_{max} as the static capacity was conservative in all cases. One case had an error less than 15 percent and the other two cases had errors less than two percent. Many additional piles had load tests which were not run to failure of the soil resistance. The piles represented in this report generally had driving resistances between 12 and 200 blows per foot. For larger blows per foot where the entire soil resistance of the pile is not mobilized, the Case Method capacity can only be expected to give the soil resistance which was mobilized. This has usually resulted in a conservative prediction as compared with the static capacity. These piles are also represented in Figure 3.11.

Chapter 4

RESISTANCE DISTRIBUTION

4.1 Description of Resistance Distribution

During Project Phase III the capability was developed to determine the magnitude and distribution of the resistance along the pile using as input, measurements of force and acceleration made at the pile top. This computational procedure can also separate the static and dynamic resistance forces using a simple model for soil resistance consisting of an elastic-plastic spring and a linear dashpot. During the current project phase no further work was done on this computational procedure and there was no opportunity to make static measurements of resistance distribution for correlation with the dynamic predictions. However, since this report represents a state-of-the-art review it is appropriate to summarize the computational algorithm and the results which have been obtained.

Consider the physical basis behind this computational method. In Figure 4.1 a drawing is shown which depicts an orthogonal view of the pile force given as a function of both pile location and time. It was obtained from dynamic measurements made at selected locations along the pile. Several lines shown were interpolated from the measured values. The particular record shown in Figure 4.1 was obtained during the testing of a special test pile at a site in Rittman, Ohio. These tests were reported in Reference 5. This record was taken after fifty feet of the pile had been driven with the pile tip in a very soft material. As can be seen there was very little resistance at the tip. The resistance that was there can be largely characterized as being dynamic or velocity dependent since it decreases later in the record as the velocity decreases. Since there is a very weak resistance at the pile tip a tension force is reflected back on the oncoming compression force creating a "valley" which progresses to the top of the pile at approximately $2L/c$ after the time of impact.

In Figure 4.2 a similar drawing is shown. It represents the same force-location-time plot based on data taken on the same pile. In this case, however, the pile had been extended an additional eight feet causing the tip to be embedded in a hard soil layer. At the time when the impact reaches the tip the force increases to a very large value which maintains itself at the pile tip for an extended period of time. There is little sign of velocity dependent resistance. Furthermore, this high resistance force reflects back to the pile top as a compression force superimposed on the oncoming compression causing an increase in the pile top force at $2L/c$ after impact. An examination of these two figures reveals that it is possible to make conclusions about the characteristics of the resistance forces merely by an examination of the force at the pile top. The Case Pile Wave Analysis Program CAPWAP, performs this in a systematic fashion.

The measured velocity obtained by integration of the acceleration record is taken as an input quantity. From this input and an assumed set of soil resistance forces, the pile top force can be computed using a lumped mass-spring system as is commonly used in all pile wave equation programs. By adjusting the resistance forces and balancing them between static and dynamic resistance it is possible to adjust the computer force so that it agrees with the measured force record. The CAPWAP program performs this function automatically. The details of the computation are beyond the scope of this report and have been reported elsewhere (Ref. 4).

The above described capability is useful for two reasons. First, it is sometimes necessary to make estimates of the resistance distribution along the pile length. There is, however, another use for this program which may be of greater value than the resistance distribution. Since a very thorough elastic dynamic analysis is performed it would be expected that the calculated total resistance force would be more reliable than values obtained by the Case Method. This has not been proven to be true based on correlation studies which have been made. However, it should be recognized that the Case Method has been calibrated by pile and soil types so that the results correlate well with the available data. If there is a large volume of previous experience on any given pile-soil

type combination then it would be expected that considerable reliability could be achieved on future sites with the same combination. In some combinations of pile type and soil type rather modest amounts of data have been used to perform this correlation and therefore it can be expected that a certain amount of difficulties may occur when the method is applied to other similar combinations. In cases such as this, experience has shown that while the CAPWAP method has not produced such high correlation values as achieved by the Case Method, it does not make a substantial unconservative error and provides considerable confidence in the predicted pile capacity.

4.2 Sample CAPWAP Results

Many piles have been tested during the past two years by project personnel. To provide a comprehensive description of each pile in this report is prohibited by the large volume of data and test experience acquired in this project phase. Therefore, only example piles will be discussed.

A 50 foot long 10HBP57 steel H pile was driven on a test site on the Purdue University campus in Lafayette, Indiana by a Delmag D-12 open end diesel hammer with a manufacture's rated energy of 22,500 ft-pounds. The soil was generally a medium sand grading gravel with depth. A gray clayey silt (ML) layer was located below the pile tip at final penetration. This test was performed in connection with the 1972 ASCE Soil Mechanics and Foundation Engineering Specialty Conference. The test results are reported in detail in Reference 25.

In addition to the standard instrumentation at the pile top, resistance strain gages were attached along the pile length. Thus, measurements of strain at five locations were made and along with two acceleration records at the pile top were recorded on two tape recorders. The dynamic records of strain in the pile as a function of time and pile length were plotted and are shown in Figure 4.3. Strain time relations for pile locations which were not measured were interpolated from the measured data. A compressive force from impact can be seen traveling at the wave speed from the pile top to the toe. Because of relatively small end

bearing forces this oncoming compression produces a tensile reflection wave which travels back toward the pile top. This tensile reflection almost completely cancels the downwards propagating hammer compression force creating a valley of near zero forces. Therefore, it can be observed that the pile top force decreases to nearly zero at approximately $2L/c$ after impact. This decrease gives an indication of the tip resistance by only observing the pile top force.

Another interesting phenomenon can be observed in Figure 4.3. The toe force, which was actually measured 1.5 feet above the pile tip, first reaches a relatively large maximum and then decreases and oscillates near 30 kips. The high peak is a result of the inertia of the 1.5 foot section and viscous damping due to the high tip velocities at this time. The average value at the later time is due to the static resistance below this point which is the same as was measured during the static load test. In general, however, static soil resistances cannot be so easily extracted from dynamic measurements at locations other than the pile toe. Intermediate locations exhibit forces due to hammer impact, static and dynamic soil resistances and pile inertia which only a detailed dynamic analysis can separate.

The static load test was run to failure at a constant rate of penetration of 0.02 inches per minute. Jack pressure, pile top displacement and the strains at the five locations along the pile length were recorded. This load test data is plotted in Figure 4.4. All forces are plotted as a function of pile top displacement. After pile yielding, the load test was run to 0.8 inches penetration. Elastic rebound was 0.22 inches. The soil resistance between gage locations can be obtained by subtracting the force readings of the two gages. In this way it is noticed that the major portion of the static soil resistance of this pile occurred between gage locations 3 and 5 which were 21 and 4 feet respectively above the pile tip.

A few blows were analyzed automatically by CAPWAP. A sample computed top force is shown in Figure 4.5 for one of the last blows during driving. Agreement is quite good with the measured forces until around $2L/c$ after

impact. Differences can be attributed to the soil model. The force distribution predicted by CAPWAP is shown in Figure 4.6b by the solid line. The measured values (at 155 kips top force) are presented by circles. In general the two distributions agree well. Figure 4.6a shows a plot of the predicted and measured load test curves. The predicted load test curve was obtained automatically using a static analysis of the resistance distribution obtained in the CAPWAP analysis.

A 12 inch O.D. with 1/4 inch wall pipe pile was driven near Oneonta, New York into a rather uniform silt (15). The standard measurements of force and acceleration were made at the pile top. A Constant Rate of Penetration (CRP) test was run two weeks after initial driving to an ultimate value of 217 kips. Dynamic data was recorded one day after the CRP test as a restrike test. The hammer used was a Vulcan #1. The pile showed increasing pile sets with continued restriking as well as a substantial strength increase over initial driving; it is logical to assume that a substantial setup effect was present.

Five selected blows were analyzed with CAPWAP. The blows were selected to reflect the loss of capacity during the early stages of re-driving and the capacity and soil resistance distribution at the end of restrike.

The results from Blow Number 1 are most important for correlation with the static test. The computed and measured forces curves are shown in Figure 4.7. Excellent agreement was achieved over all time. The agreement of the predicted capacity (204 kips) with the static test is also good. The measured load test and CAPWAP predicted load test are shown in Figure 4.8a with close agreement. The curve in Figure 4.8b for Blow Number 1 can be interpreted as follows. There is a zero force in the pile at the bottom. About sixteen feet above the pile tip the force is 76 kips. This means that a soil resistance of 76 kips acts over the bottom 16 feet of the pile. The rest of the static soil resistance ($204 - 76 = 128$ kips) acted in a relatively uniform manner along the upper 69 feet of the pile. Thus, the pile is mainly a friction pile. The maximum total dynamic resistance for this blow was 93 kips or

46 percent of the static prediction.

The other blows analyzed for this pile show a rapid capacity breakdown with increasing blow number. Also the resistance distribution changes rapidly from side friction to toe resistance with an increase of toe resistance. This distribution change is apparent even in the second blow and by blow 8 the static capacity of only 89 kips was entirely end bearing. Such dramatic changes in so few blows can only be studied from such measurements, either by an analysis similar to CAPWAP or by measurements along the pile length as in the Purdue test. The maximum dynamic resistance for Blow 8 was 231 kips or 260 percent of the static capacity. The static capacity continued to decrease to a value of 65 kips for Blow 122, the last blow analyzed. It is impossible to ascertain whether or not the static capacities are correct for these later blows with the large dynamic to static ratios. It would seem that for such high ratios that the simple Case Method cannot yield a sufficiently reliable result. On the other hand the linear viscous damping model used in CAPWAP is also only an approximation.

The entire Case Project approach to pile driving was originally developed and tested exclusively on the pile types which were commonly used in the state of Ohio, namely steel piles. In order for the procedure to be completely general, the method should also work well on other pile types. The testing of timber and concrete piles were performed in cooperation with other highway departments. The results which were obtained indicated that the procedure worked and that the method was independent of the pile type.

A timber pile with a non-uniform cross section was tested near Monticello, Minnesota with a Linkbelt 440 hammer (13). The soil was a rather uniform sand with silt layers. The ultimate capacity from the CRP test was 132 kips. Data was taken during the last 170 blows of driving. Five blows were analyzed with CAPWAP, three from early records and two at the end of driving. Plots of predicted and measured force curves are shown in Figure 4.9 and 4.10 for early and late blows respectively. The match is generally very good except at about $2L/c$ after impact.

The load test curve predicted from CAPWAP for the blow at the end of driving shows good agreement with the CRP test curve as shown in Figure 4.11a.

The resistance distribution for all five blows is shown in Figure 4.11b. The early blows showed capacities of about 90 kips, and the predicted capacities of the last blows was around 120 kips. This indicated capacity buildup was also noted in the field by increased driving resistance. As can be seen no resistance was found to act above grade as should be expected. For Blow II-135, 80 kips is the force in the pile 2.5 feet above the tip. This means 44 kips (124-80) resistance along the skin with rather uniform distribution. Thus, about 2/3 of the total resistance was end bearing.

Due to the reduced availability and increased cost of steel piling, prestressed concrete piles are becoming more economical throughout the country. A test was performed in Miami, Florida on 18 inch solid section prestressed piles driven with a Delmag D-30 hammer (19). Dynamic data on the load test pile was taken after the CRP test had failed at 358 kips. The CAPWAP force match, in Figure 4.12, agreed well. The predicted capacity of 372 kips agrees well with the measured value and the measured and CAPWAP predicted load test curves show satisfactory agreement as seen in Figure 4.13a. The resistance distribution shown in Figure 4.13b shows very little static capacity along the upper 2/3 of the pile length.

While such results for the prestressed pile presented here are interesting and show the method to be applicable, further tests on 60 foot long, 18 inch concrete piles at this site show another interesting application of the CAPWAP analysis. Current specifications for the driving of prestressed concrete piles try to prohibit the cracking of the concrete during impact by controlling the hammer properties. Because the pile tip resistance is smaller than the impact force, the impact compression force reflects at the pile tip and returns as a tensile force. If the reflected tensile force is larger than the oncoming compression force a net tensile force can occur which, if large enough, can cause structural damage in the form of tensile cracks. The CAPWAP analysis,

because it can compute the effects of impact, reflections and soil forces and their time of arrival at various locations along the pile length, can also produce a predicted force-time-pile length curve similar to that measured in Purdue. The only inputs required are the measured top force and acceleration which are necessary (and easy to perform using the current system) for the Case procedures. The computer can then find the location and magnitudes of the most critical tensile and compressive stresses. Because of Florida's interest in tensile stresses, strain measurements were also made at the mid length of these piles. Comparisons of the measured stresses at this location with that predicted by CAPWAP for the same location from measurements taken at the pile top for easy and medium driving resistances are shown in Figures 4.14 and 4.15 respectively. Agreement of the maximum stress magnitudes is excellent. In addition, the stress-time curves also match quite well. Thus, it can be concluded that driving stresses for all pile locations can be accurately predicted from measurements made only at the pile top. CAPWAP then becomes an effective tool for investigating impact induced structural damage.

Chapter 5

Conclusions

1. The instrumentation developed during the course of the project provides a reliable and accurate means of measuring force and acceleration at the pile top during driving. These measurements can be made on a routine basis requiring only a very short interruption of the contractor's operation.

2. Using the automatic processing system developed by the project a large number of hammer blows can be processed and analyzed. Useful driving parameters such as pile top energy, maximum velocity, maximum force, etc. can be easily calculated and printed. Also computer controlled plots of the driving record can be made automatically from the digital record.

3. The Case Method capacity using time delay gives an excellent correlation with statically measured values.

4. The Case Method capacity using a soil dependent damping constant also shows good agreement with the statically measured value. It has the advantage of greater rationality compared with the time delay approach and, in addition, conservatism can be achieved at the judgement of the engineer by use of a larger damping constant.

5. The CAPWAP procedure can obtain the resistance distribution and can separate the static and dynamic resistances using the dynamic pile top measurements only. While the results show a somewhat larger correlation coefficient with the static measurements than does the Case Method, the improved model used to describe the soil and the pile should be expected to produce better results in unfamiliar conditions.

6. CAPWAP can also be used to evaluate particular problems of driving stresses.

7. Limited implementation has been achieved and the application of this work is expanding rapidly.

APPENDIX A

Derivation of J_c

Replacing the pile by a mass-spring-damper system Newton's Second Law becomes

$$m \ddot{x}(t) + b \dot{x}(t) + k x(t) = F(t) \quad (A1)$$

If we now define (26)

$$\zeta = \frac{b}{2m\omega_n} \quad \text{and} \quad \omega_n^2 = \frac{k}{m} \quad (A2)$$

where ζ is the viscous damping factor and b is the coefficient of viscous damping, then

$$\zeta = \frac{b}{\sqrt{mk}} \quad (A3)$$

where, for the pile, the mass m is ρAL and the stiffness k is $\frac{EA}{L}$.
Recalling Equation 3.14, the value for ζ becomes

$$\zeta = \frac{bc}{2EA} \quad (A4)$$

and is critically damped when

$$b_{cr} = \frac{2EA}{c} \quad (A5)$$

introducing $J_c = 2\zeta$ we get

$$b = J_c \frac{EA}{c} \quad (A6)$$

for $0 < J_c < 2$.

REFERENCES

1. Eiber, R. J., "A Preliminary Laboratory Investigation of the Prediction of Static Pile Resistances in Sand", Master's Thesis, Dept. of Civil Engineering, Case Institute of Technology, 1958.
2. Goble, G. G., Scanlan, R. H. and Tomko, J. J., "Dynamic Studies on the Bearing Capacity of Piles", Vol. I and II, Case Institute of Technology, July 1967.
3. Goble, G. G., Tomko, J. J., Rausche, F. and Green, P. M., "Dynamic Studies on the Bearing Capacity of Piles, Phase II", Vol. I and II., Report No. 31, Division of Solid Mechanics, Structures and Mechanical Design, Case Western Reserve University, July, 1968.
4. Goble, G. G., Rausche, F., and Moses, F., "Dynamic Studies on the Bearing Capacity of Piles, Phase III", Report No. 48, Division of Solid Mechanics, Structures and Mechanical Design, Case Western Reserve University, 1970.
5. Goble, G. G., Scanlan, R. H. and Tomko, J. J., "Dynamic Studies on the Bearing Capacity of Piles", Highway Research Record, Number 167, Highway Research Board, Washington, D. C., 1967.
6. Goble, G. G. and Rausche, F., "Pile Load Test by Impact Driving", paper presented to the Highway Research Board Annual Meeting, Washington, D. C., January 1970.
7. Rausche, F., Goble, G. G., and Moses, F. "A New Testing Procedure for Axial Pile Strength", Third Annual Offshore Technology Conference, Paper No. OTC 1481, Houston, Texas, 1971.
8. Goble, G. G., Fricke, K. and Likins, G. E., "Driving Stresses in Concrete Piles", to be published in PCI Journal, Nov.-Dec. 1975.
9. Goble, G. G. and Rausche, F., "Dynamic Measurements of Pile Behavior", Proceedings of the Conference on Design and Installation of Pile Foundations and Cellular Structures, Lehigh University, April, 1970.
10. Goble, G. G., Moses, F. and Rausche, F., "Prediction of Pile Behavior from Dynamic Measurements", Proceedings of the Conference on Design and Installation of Pile Foundations and Cellular Structures, Lehigh University, April 1970.
11. Goble, G. G., Walker, F., and Rausche, F., "Pile Bearing Capacity - Prediction vs. Performance", Proceedings of the Specialty Conference on Performance of Earth and Earth-Supported Structures, Vol. I, Part 2, Purdue University, Lafayette, Indiana, June 1972.

12. Goble, G. G. and Rausche, F., "A Static and Dynamic Pile Test in Pocatello, Idaho", Division of Solid Mechanics, Structures and Mechanical Design, Case Western Reserve University, Cleveland, Ohio June 1971.
13. Goble, G. G. and Raushce, F., "A Static and Dynamic Timber Test Pile Test in Monticello, Minnesota", Division of Solid Mechanics, Structures and Mechanical Design, Case Western Reserve University, Cleveland, Ohio, December 1971.
14. Goble, G. G. and Rausche, F., "Static and Dynamic Tests on Two Pipe Piles in Philadelphia, Pennsylvania", Division of Solid Mechanics, Structures and Mechanical Design, Cleveland, Ohio, January 1972.
15. Goble, G. G. and Likins, G. E., Jr., "A Static and Dynamic Pile Test in Oneonta, New York", Division of Solid Mechanics, Structures and Mechanical Design, Cleveland, Ohio, April 1972.
16. Goble, G. G. and Likins, G. E., Jr., "A Static and Dynamic Pile Test in Whitehall, New York", Department of Solid Mechanics, Structures and Mechanical Design, Cleveland, Ohio, August 1973.
17. Goble, G. G. and Likins, G. E., Jr., "A Static and Dynamic Pile Test in West Palm Beach, Florida", Department of Solid Mechanics, Structures and Mechanical Design, Cleveland, Ohio, August 1973.
18. Goble, G. G., and Likins, G. E., Jr., "Predicting the Bearing Capacity of a Pile from Dynamic Measurements in Tarver, Georgia", Department of Solid Mechanics, Structures and Mechanical Design, Cleveland, Ohio, February 1974.
19. Goble, G. G., Fricke, K. E., Likins, G. E., Jr., "A Static and Dynamic Pile Test in Dade County, Florida", Department of Solid Mechanics, Structures and Mechanical Design, Cleveland, Ohio, March 1974.
20. Goble, G. G. and Fricke, K. E., "A Static and Dynamic Pile Test in Tallahassee, Florida", Department of Solid Mechanics, Structures and Mechanical Design, Cleveland, Ohio, December 1973.
21. Goble, G. G., and Likins, G. E., Jr., "A Static and Dynamic Pile Test in Fairmount, Minnesota", Department of Solid Mechanics, Structures and Mechanical Design, Cleveland, Ohio, July 1974.
22. Michigan State Highway Commission, "A Performance Investigation of Pile Driving Hammers and Piles", Final Report, Lansing, Michigan, March 1965.
23. Timoshenko, S. P. and Goodier, J. N., Theory of Elasticity, McGraw-Hill Book Company, Third Edition, New York, 1970.
24. Smith, E. A. L., "Pile Driving Analysis by the Wave Equation", Journal of the Soil Mechanics and Foundations Division, Proceedings of the ASCE, Paper 2574, SM4, August 1960, pp. 35-61.

25. Goble, G. G., Kovacs, W. D., and Rausche, F., "Field Demonstration: Response of Instrumented Piles to Driving and Load Testing", Proceedings of the Specialty Conference on Performance of Earth and Earth-Supported Structures, Volume III, Purdue University, Lafayette, Indiana, June 1972.
26. Meirovitch, Leonard, Analytical Methods in Vibration, MacMiller Co., New York, 1967.

<u>Number</u>	<u>Name</u>	<u>Date</u>	<u>Hammer</u>	<u>Pile Type</u>	<u>Pile Length</u>	<u>Tip Soil</u>	<u>Side Soil</u>
1	91A	6-66	V1	12" CIP	76.5	silty clay	
2	692	8-66	LB520	18" CIP	76	silty clay	
3	C1	1-67	D12	12" monotube	59	sandy gravel	
4	F30	6-67	LB440	12" CIP	33	sandy silt	
5	F50	6-67	LB440	12" CIP	51.5	silt	
6	F50A	7-67	LB440	12" CIP	51.5	silt	
7	F60	7-67	LB440	12" CIP	60.5	silt	
8	F60A	7-67	LB440	12" CIP	60.5	silt	
9	CIN 68	1-68	D12	12" CIP	66	gravelly sand	
10	272	4-68	LB440	12" CIP	57.5	sandy silt, stone	silty clay
11	T050	9-68	D12	12" CIP	48	silty clay	silt
12	T050A	9-68	D12	12" CIP	48	silty clay	silt
13	T060	9-68	D12	12" CIP	60	silty clay	silt
14	T060A	9-68	D12	12" CIP	60	silty clay	silt
15	Logan	11-68	D12	12" CIP	58	silty gravelly sand	
16	W56	6-69	D12	12" CIP	56.3	clay	
17	W76	6-69	D12	12" CIP	78.2	clay	
18	CH41	8-69	D12	12" CIP	41	gravelly sand	
19	RI50	1-70	D12	12" CIP	50	silty clay	

TABLE 2.1

<u>Number</u>	<u>Name</u>	<u>Date</u>	<u>Hammer</u>	<u>Pile Type</u>	<u>Pile Length</u>	<u>Tip Soil</u>	<u>Side Soil</u>
20	RI50A	1-70	D12	12" CIP	50	silty clay	
21	CR7-74	1-71	LB520	14/12.5/11 CIP	75	silt	silty clay
22	CR5-72	1-71	LB520	14/12.5/11 CIP	80	clayey silt	
23	CR6-52	2-71	LB520	14/12.5/11 CIP	90	clayey silt	silt, silty clay
24	TO73	3-71	LB440	12" CIP	47	gray gravelly silty clay	
25	Idaho	3-71	LB312	16" CIP	46	sand	silty clay
26	CP1	5-71	LB520	12" CIP	46	sand	fill
27	CR1-63	8-71	LB520	14/12.5/11 CIP	103	gray silt & clay	
28	Monticello	9-71	LB440	Timber	30	fine sand & silt layers	
29	PHIL77	11-71	V-1	12" CIP	45	sand, gravel	silt, clay, peat
30	PHIL78	11-71	V-1	12" CIP	43	fine sand	silt, clay, peat
31	CIN 14.5	1-72	LB440	12" CIP	42	gray still silty clay	
32	CIN 170	1-72	LB440	12" CIP	52	gray still silty clay	
33	Oneonta	2-72	V1	12" CIP	86.5	silt	
34	Purdue	6-72	D12	10HBP57	50	silt & gravel	sand, gravel
35	CP2	7-72	C5	Timber	49	M-F brownish gray sand	sand, silt
36	CP3	7-72	V1	Timber	49	fine light brown sand, trace silt	
37	CP4	7-72	C5	Timber	49	F-VF dark brown sand, trace silt	sand, silt, peat

TABLE 2.1 (Cont.)

<u>Number</u>	<u>Name</u>	<u>Date</u>	<u>Hammer</u>	<u>Pile Type</u>	<u>Pile Length</u>	<u>Tip Soil</u>	<u>Side Soil</u>
38	TP 4-5	9-72	D-30	12-3/4" CIP	61	compact brown fine-coarse silty sand & gravel [SM]	
39	TP 5-5	9-72	D-30	10HP57	75	fine-coarse light brown silty sand, some gravel [SM]	
40	TP 1-5	9-72	D-30	Timber	45	dark green medium-coarse sand, some gravel [SW]	
41	CP5	10-72	D22	12" CIP	59	clay till	
42	GA	10-72	DE-30	16" CIP	39.7	med dense gray clayey sandy silt [SC]	
43	TP 6-1	11-72	D-30	12" PSC	66	interbeds of gray silty clay and fine-medium sand [CL-SM]	
44	TP 1-1A	11-72	D-30	Timber	50	compact greenish gray fine to coarse sand [SW]	43 silty sand & clay
45	TP 4-1A	11-72	D-30	12-3/4" CIP	104	soft black organic clay [CH]	
46	TP 4-5A	11-72	D-30	12-3/4" CIP	70	compact brown fine-coarse silty sand & gravel [SM]	
47	TP 5-5A	11-72	D-30	10HP57	79	fine-coarse light brown silty sand, some gravel [SM]	
48	TP 1-5A	11-72	D-30	Timber	45	dark green medium-coarse sand, some gravel [SW]	

TABLE 2.1 (Cont.)

<u>Number</u>	<u>Name</u>	<u>Date</u>	<u>Hammer</u>	<u>Pile Type</u>	<u>Pile Length</u>	<u>Tip Soil</u>	<u>Side Soil</u>
49	Whitehall	1-73	V 06	14" PSC	140	firm gray silt & clay	very soft gray silt & clay
50	CP6	3-73	H-39	11.4" PSC	49.2'	gray coarse sand with shells	peat, clay, fine sand
51	CP7	3-73	H-39	11.4" PSC	49.2'	gray coarse sand, with shells	peat, clay, fine sand
52	CP8	3-73	H-39	11.4" PSC	49.2'	gray coarse sand with shells	peat, clay, fine sand
53	CP9	3-73	LB660	12-3/4" CIP	75	clayey sand, till [SC]	[SP-SM-SC]
54	WPB1	4-73	F20	18" PSC	45	light gray sand & shell	
55	WPB2	4-73	F20	18" PSC	35	light gray sand & shell	
56	CP10	4-73	65C	14" PSC	74	silty fine sand	
57	CP11	5-73	65C	Timber	63	firm sand, clayey silt layers	
58	CP12	5-73	65C	10" PSC	73	firm sand, clayey silt layers	
59	Tallahassee	5-73	F20	18" PSC	40	yellow sand & clay	
60	Miami 1	7-73	D-30	18" PSC	25	white Oolitic limerock	
61	Miami 2	7-73	D-30	18" PSC	35	white sandy limerock & shell	
62	Fair A	8-73	D-15	Timber	29	clay, till	
63	Fair D	8-73	D-15	Timber	33	clay, till	
64	CIN I471	10-73	LB440	12" CIP	48	gray silty clay	silts

<u>Number</u>	<u>Name</u>	<u>Date</u>	<u>Hammer</u>	<u>Pile Type</u>	<u>Pile Length</u>	<u>Tip Soil</u>	<u>Side Soil</u>
65	CR10E	1-74	LB520	12" CIP	53	clayey silt	sands & silts
66	CP13	1-74	K13	12" monotube	50	snad, till	
67	CP14	2-74	K25	12-3/4" CIP	99	fine sand, silt lenses [SP]	
68	CP15	2-74	K25	14" PSC ^{oct}	100	medium grained sand [SP]	
69	CP16	2-74	K25	14" PSC ^{oct}	100	fine sand, silt lenses [SP]	
70	CP17	2-74	K25	16" CIP	104	medium grained sand [SP]	
71	Maine 1	2-74	DE20	10" CIP	45	loose fine gray silty micaceous sand	
72	Maine 2	3-74	DE20	10" CIP	45	loose fine gray silty micaceous sand	45
73	CP18	3-74	D22	16" monotube	128	very dense fine sand, gravel, boulders [SP-SM]	sand [SP]
74	CP19	5-74	D-30	18" PSC	24.8	sand	

TABLE 2.1 (Cont.)

TABLE 2.1a

Number	Name	Pile Area in ²	Blow Count Blows/Foot	Static Test Result kips	Case Method Predictions			
					J Capacity	δ (%)	Time Delay Capacity	
1	91A	7.8	25	264	.55	261	25	232
2	692	14.5	67	300	.55	351	-	NA
3	C1	5.8	44	184	.05	201	0	210
4	F30	9.8	30	87	.3	101	140	108
5	F50	9.8	60	194	.3	170	25	166
6	F50A	9.8	480	218	.3	233	25	237
7	F60	9.8	96	180	.3	217	25	221
8	F60A	9.8	144	218	.3	208	25	217
9	CIN 68	6.7	46	160	.05	176	0	179
10	272	6.7	>200	194	.2	218	25	232
11	T050	9.8	16	47	.55	40	140	71
12	T050A	9.8	NA	92	.55	153	140	99
13	T060	9.8	57	39	.55	43	140	57
14	T060A	9.8	NA	81	.55	145	140	110
15	LOGAN	6.7	46	210	.15	206	0	226
16	W56	6.7	52	94	1.1	113	140	67
17	W76	6.7	100	163	1.1	163		NA
18	CH41	6.7	50	180	.05	200	0	205
19	RI50	9.3	NA	37	.55	32	140	58
20	RI50A	9.3	NA	60	.55	54	140	52
21	CR7-74	9.5	57	390	.3	391	25	362
22	CR5-72	8.8	47	279	.55	263	25	242

TABLE 2.1a (cont.)

Number	Name	Pile Area in ²	Blow Count Blows/Foot	Static Test Result kips	Case Method Predictions			
					J	Damping Capacity	Time Delay Capacity	
23	CR6-52	8.8	400	262	.55	251	25	251
24	T073	6.7	134	192	.55	192	25	195
25	IDAHO	18.6	52	390	.05	389	0	393
26	CPI (Bentley)	6.7	>200	280	.05	238	0	237
27	CR1-63	9.5	156	286	.55	286	25	269
28	MONTICELLO	98	27	130	.15	122	0	125
29	PHIL 77	7.1	72	230	.05	195	0	199
30	PHIL 78	7.1	48	155	.05	148	0	152
31	CIN 14.5	6.7	41	182	1.1	159		NA
32	CIN 170	6.7	70	147	1.1	162	140	117
33	ONEONTA	9.6	10	221	.3	248	25	213
34	PURDUE	19.2	40	166	.15	164	150	160
35	CP2	144.0	38	164	.05	158	0	140
36	CP3	111.0	20	196	.05	161	25	182
37	CP4	160.0	30	105	.05	95	150	86
38	TP 4-5	19.2	20	282	.05	238	25	236
39	TP 5-5	16.8	11	210	.10	196	150	200
40	TP 1-5	161.0	19	280	.05	263	0	285
41	CP5	6.7	27	136	1.1	125	40	133
42	GA	12.8	96	260	.3	288	140	240
43	TP6-1A	143.0	23	260	.2	266	150	237
44	TP1-1A	177.5	24	350	.05	377	0	325

TABLE 2.1a (cont.)

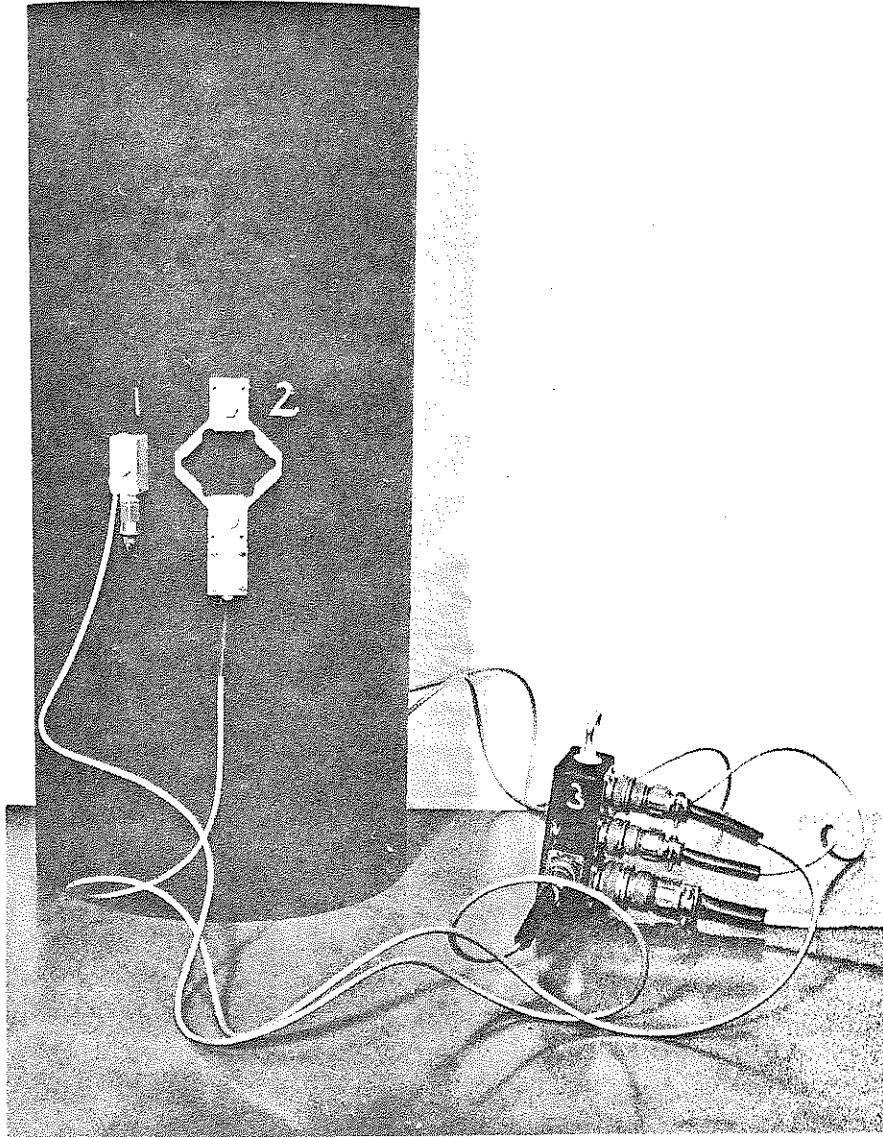
Number	Name	Pile Area in ²	Blow Count Blows/Foot	Static Test Result kips	Case Method Predictions			
					J	Damping Capacity	Time Delay Capacity	
45	TP4-1A	12.2	6	380	1.1	280	25	401
46	TP4-5A	16.9	20	282	.15	220	25	277
47	TP5-5A	16.8	11	210	.10	181	150	197
48	TP1-5A	161.0	19	280	.1	335		NA
49	WHITEHALL	196.0	127	150	1.1	118	25	143
50	CP6	130.0	89	252	.05	256		NA
51	CP7	190.0	224	450	.05	439		NA
52	CP8	190.0	238	480	.05	521		NA
53	CP9	19.2	110	578	.15	525	0	564
54	MPB 1	324.0	114	234	.05	197	25	233
55	MPB 2	324.0	59	170	.05	148	25	164
56	CP10	196.0	76	320	.15	278	25	312
57	CP11	144.0	57	233	.2	231	0	217
58	CP12	100.0	58	176	.2	195	25	173
59	TALLAHASSEE	324.0	276	328	.3	317	25	336
60	MIAMI 1	324.0	12	437	.10	484	25	388
61	MIAMI 2	324.0	18	358	.10	376	25	384
62	FAIR A	132.8	60	169	1.1	184	100	160
63	FAIR D	151.7	24	146	1.1	125	25	152
64	CIH I471	7.0	150	180	.55	173	0	204
65	CR 10E	8.1	42	140	.55	146	140	157
66	CP 13	7.0	50	382	.05	374	0	377

TABLE 2.1a (cont.)

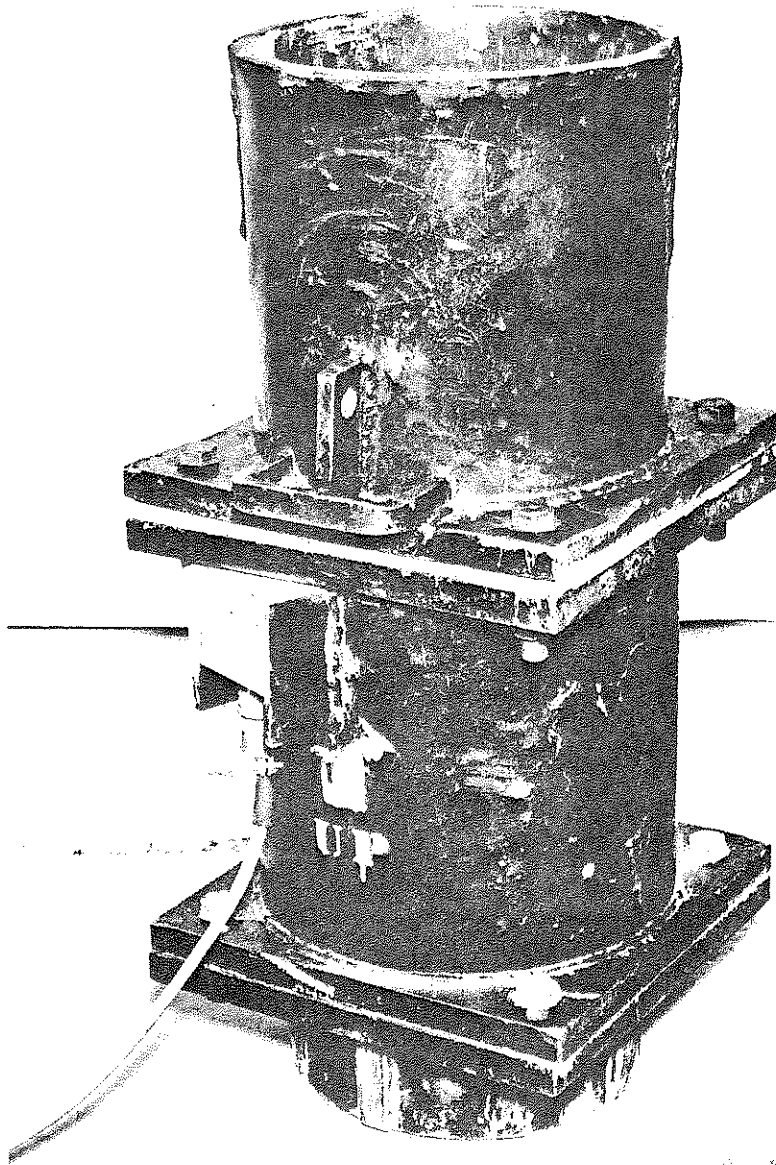
Number	Name	Pile Area in ²	Blow Count Blows/Foot	Static Test Result kfps	Case Method Predictions		
					J	Damping Capacity	Time Delay Capacity
67	CP 14	9.8	42	310	.15	326	NA
68	CP 15	162.0	56	470	.05	535	NA
69	CP 16	162.0	82	440	.25	545	NA
70	CP 17	18.4	32	440	.05	392	NA
71	MAIN 1	10.0	~ 12	32	.2	41	NA
72	MAIN 2	10.0	~ 14	42	.2	64	NA
73	CP 18	10.8	132	512	.05	469	NA
74	CP 19	314.0	152	550	.05	578	NA

Hammer	Rated Energy [FT-LB]	Ram Weight [LB]	Type
DeImag D12	22,500	2750	Open end diesel
DeImag D15	27,100	3300	Open end diesel
DeImag D22	39,700	4850	Open end diesel
DeImag D30	54,250	6600	Open end diesel
Fairchild F20	20,000	6667	Single acting air steam
Hera H39	45,600	4950	Open end diesel
Kobe K13	25,200	2870	Open end diesel
Kobe K22	41,300	4850	Open end diesel
Kobe K25	50,700	5510	Open end diesel
Kobe K60	105,600	13200	Open end diesel
Linkbelt LB312	15,000	3857	Closed end diesel
Linkbelt LB440	18,200	4000	Closed end diesel
Linkbelt LB520	26,300	5070	Closed end diesel
Linkbelt LB660	45,000	7560	Closed end diesel
McKiernan-Terry C5	16,000	5000	Double acting air steam
McKiernan-Terry DE20	16,000	2000	Open end diesel
Raymond 65c	19,500	6500	Differential steam
Vulcan V1	15,000	5000	Single acting air steam
Vulcan V06	19,500	6500	Single acting air steam

TABLE 2.1 (cont.)



2.1 Photograph of lightweight accelerometer (1) and strain transducer (2) bolted to steel pipe section. An identical transducer set is bolted to the other side and all wires are connected to connection box (3) with single cable then leading to electronic recording system.



2.2 Photograph of Case force transducer for 12 inch pipe piles. Accelerometers also are attached to inside of the force transducer.

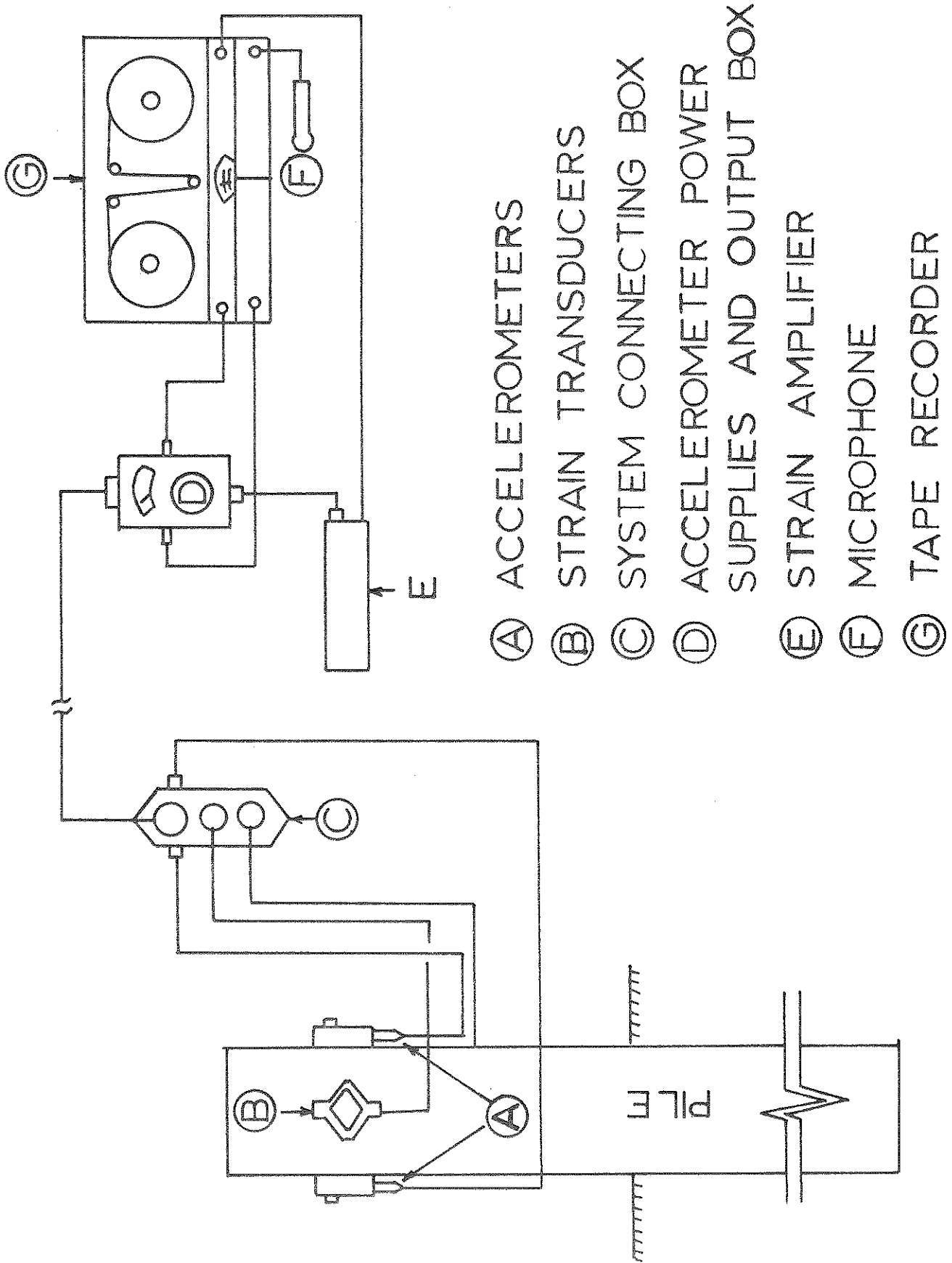
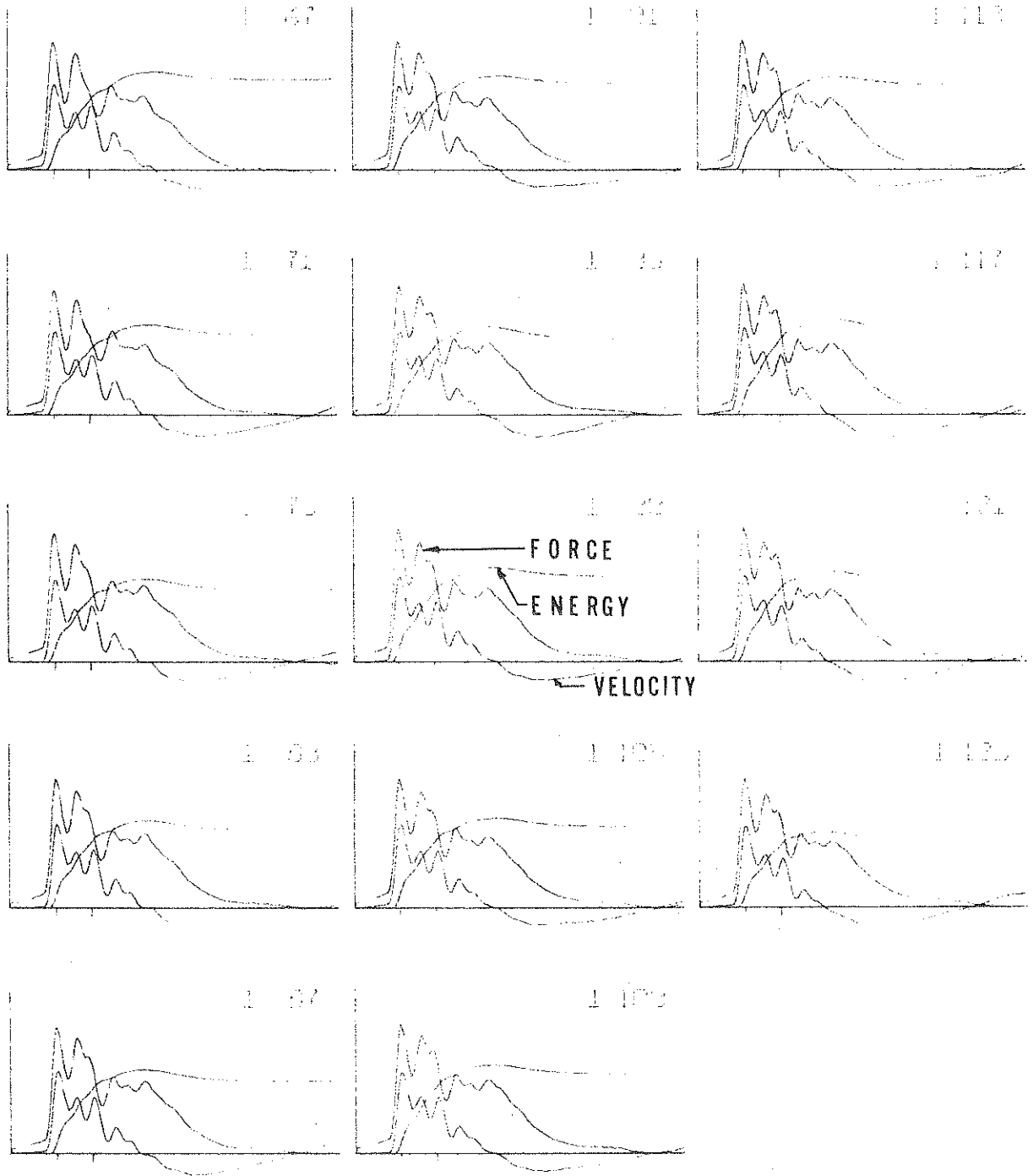


Figure 2.5: Schematic of transducer attachment and data acquisition system.



TIME 25msec inch
 VELOCITY 25 ft sec inch
 ENERGY 25 k-ft inch
 FORCE 300 kips inch

FAIRMOUNT

Figure 2.4: Sample dynamic records plotted automatically by Case Processing system

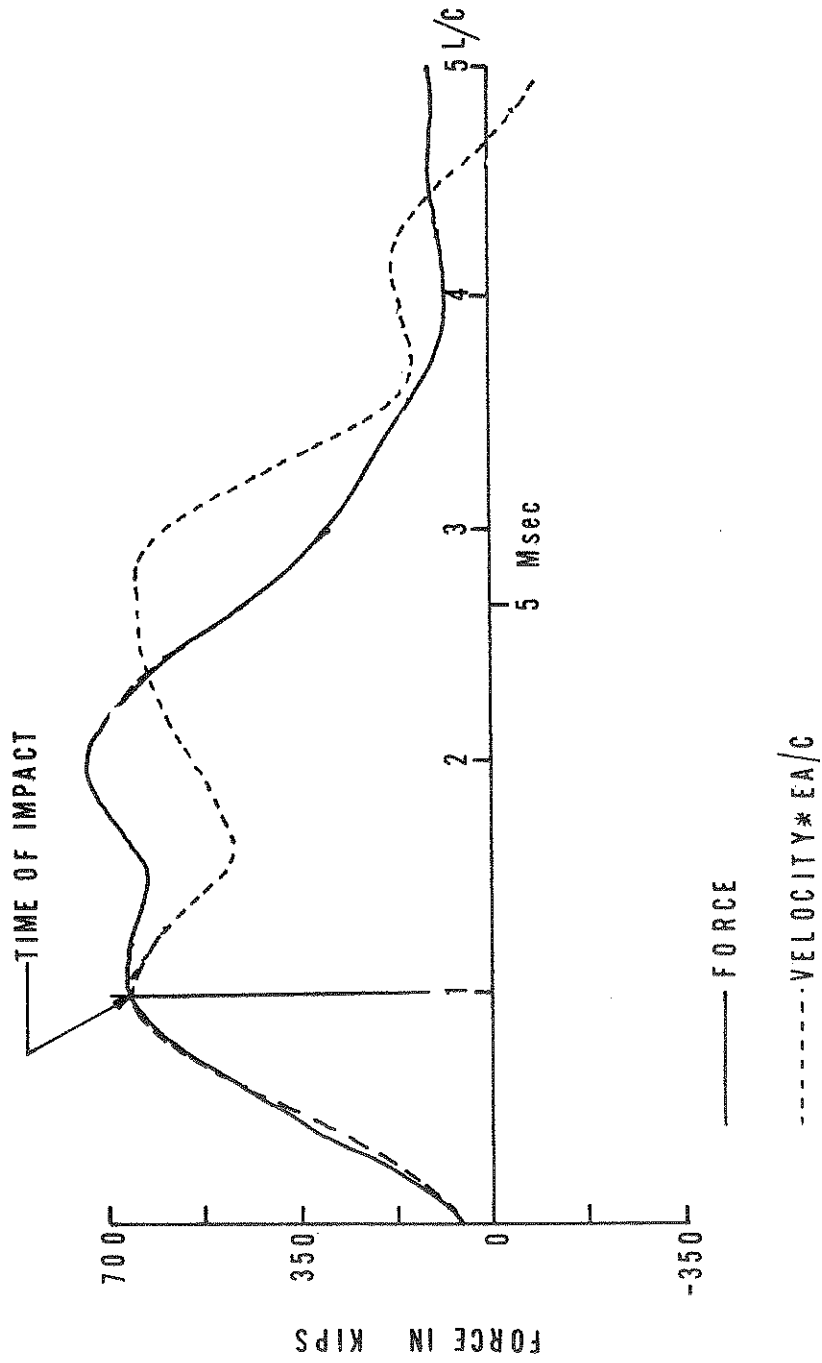


Figure 3.1: Sample dynamic record from a square 18 inch prestressed concrete pile 25 feet long.

$$V(t) = \frac{c}{EA} \sum_{i=1}^n R_i \left[2m + H \left(t - \frac{2x_i + 2mL}{c} \right) \right]$$

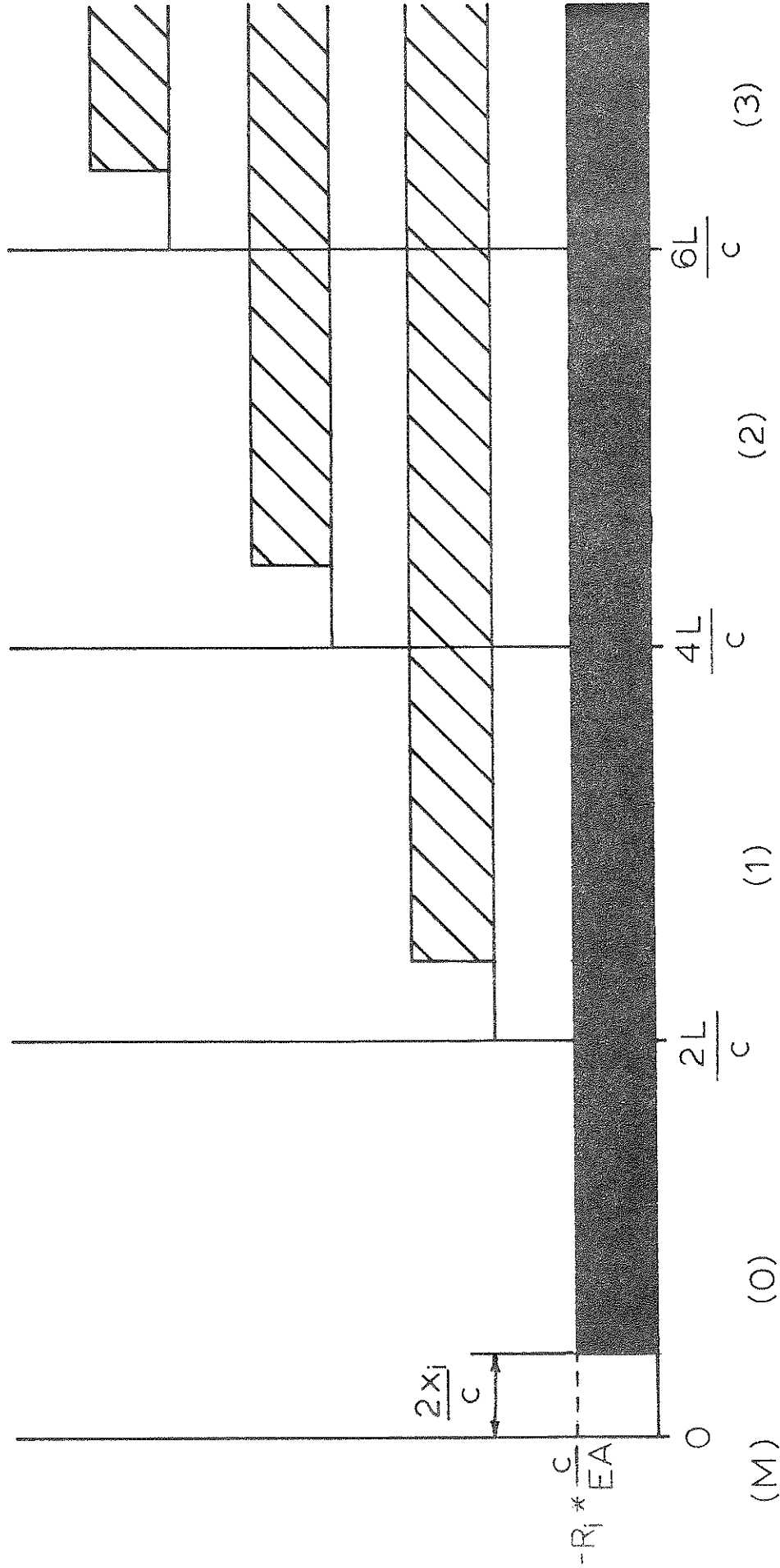


Figure 3.2: Velocity effect at pile top caused by a resistance step force R_i at location X_i from top.

$$R = \frac{F(T^*) + F(T^* + 2L/C)}{2} + \frac{MC}{2L} [V(T^*) - V(T^* + 2L/C)]$$

$$R = \frac{188 + 178}{2} - 6.4 [3.5 - (-0.5)]$$

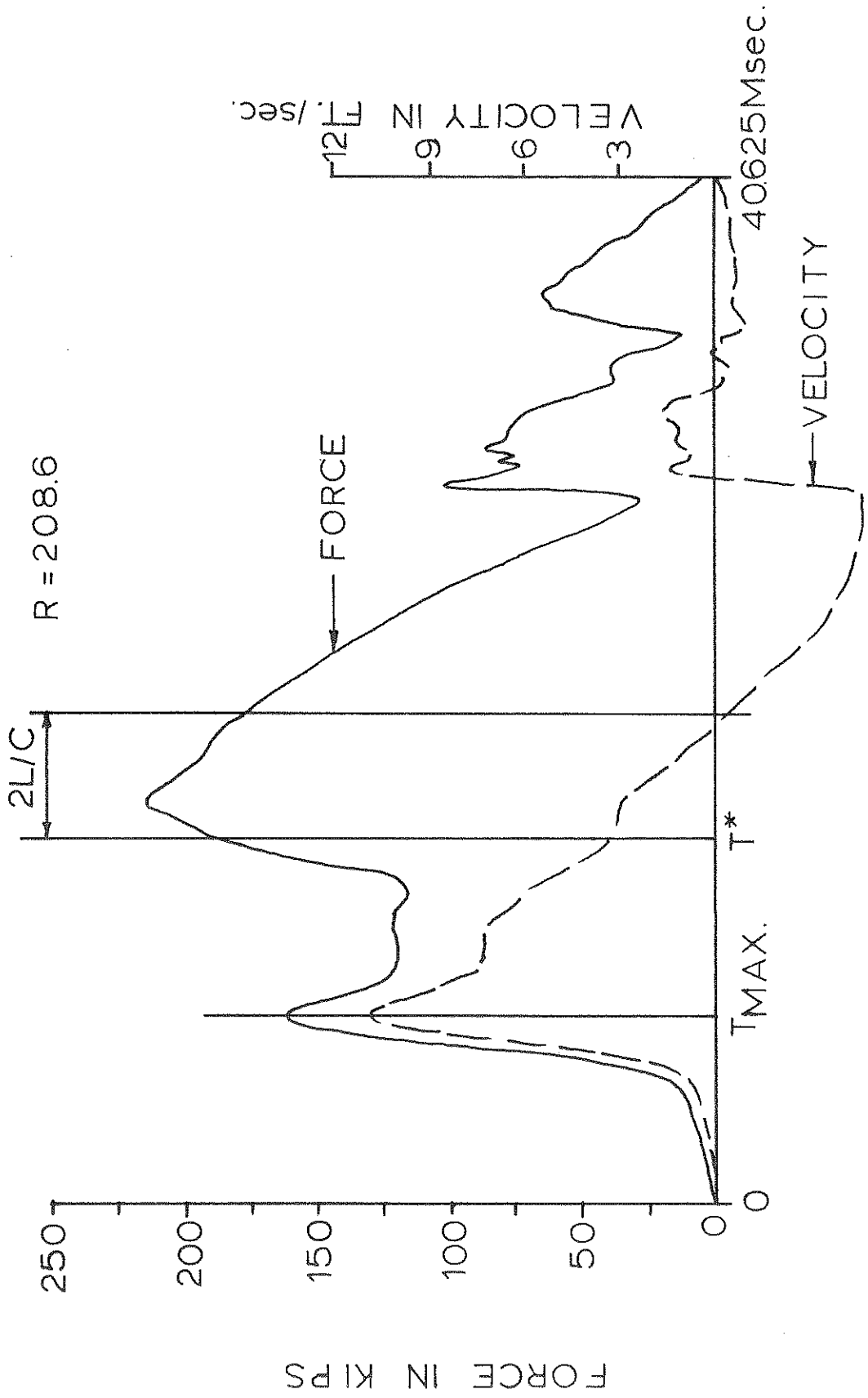


FIGURE 3.3: Sample dynamic record and Case Method computation (12 inch O.D., .179 inch wall C.I.P. pile 43.5 feet long)

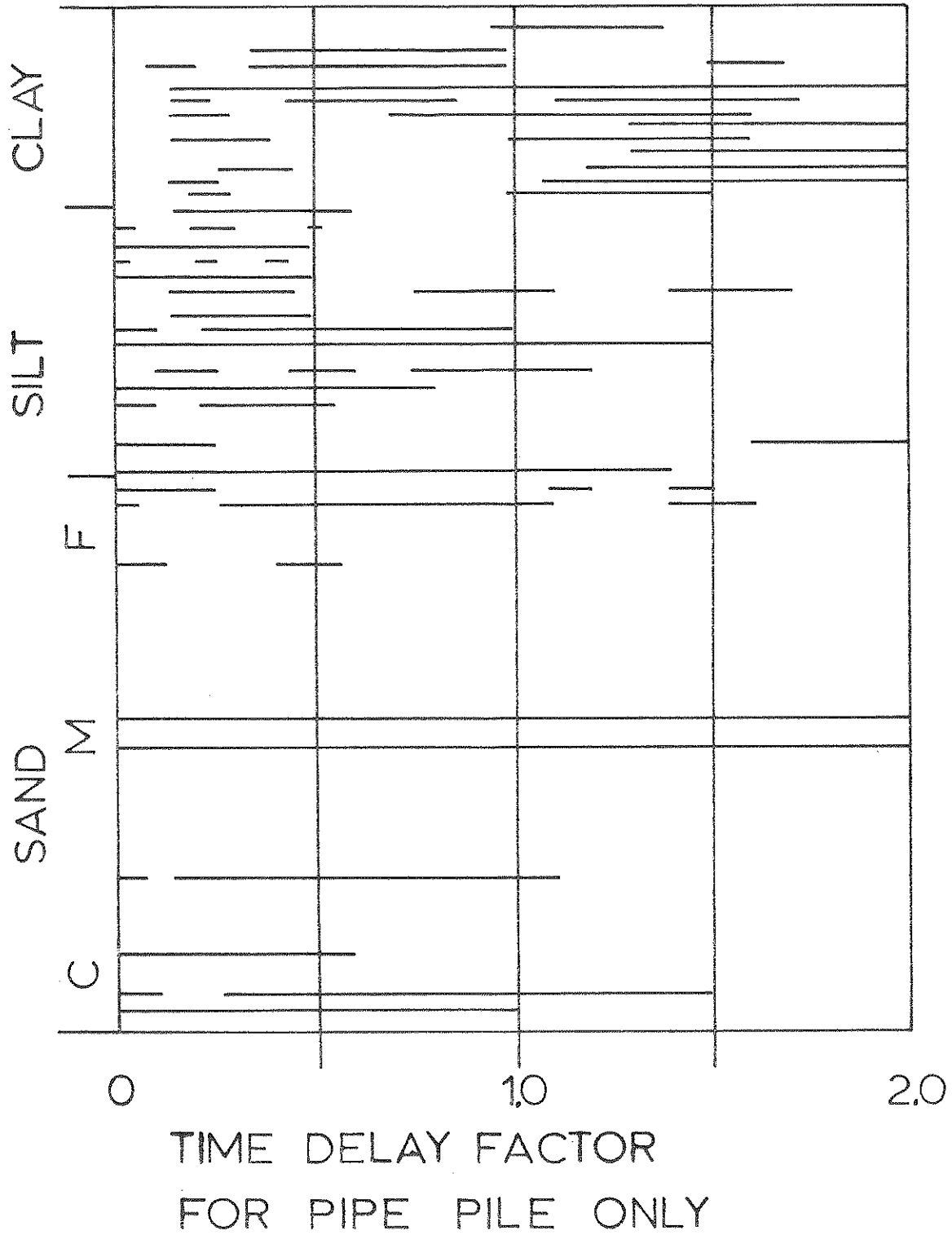


Figure 3.4: Time delay factor versus soil type at the pile tip giving prediction within 15% of load test.

ALL PILE TYPES

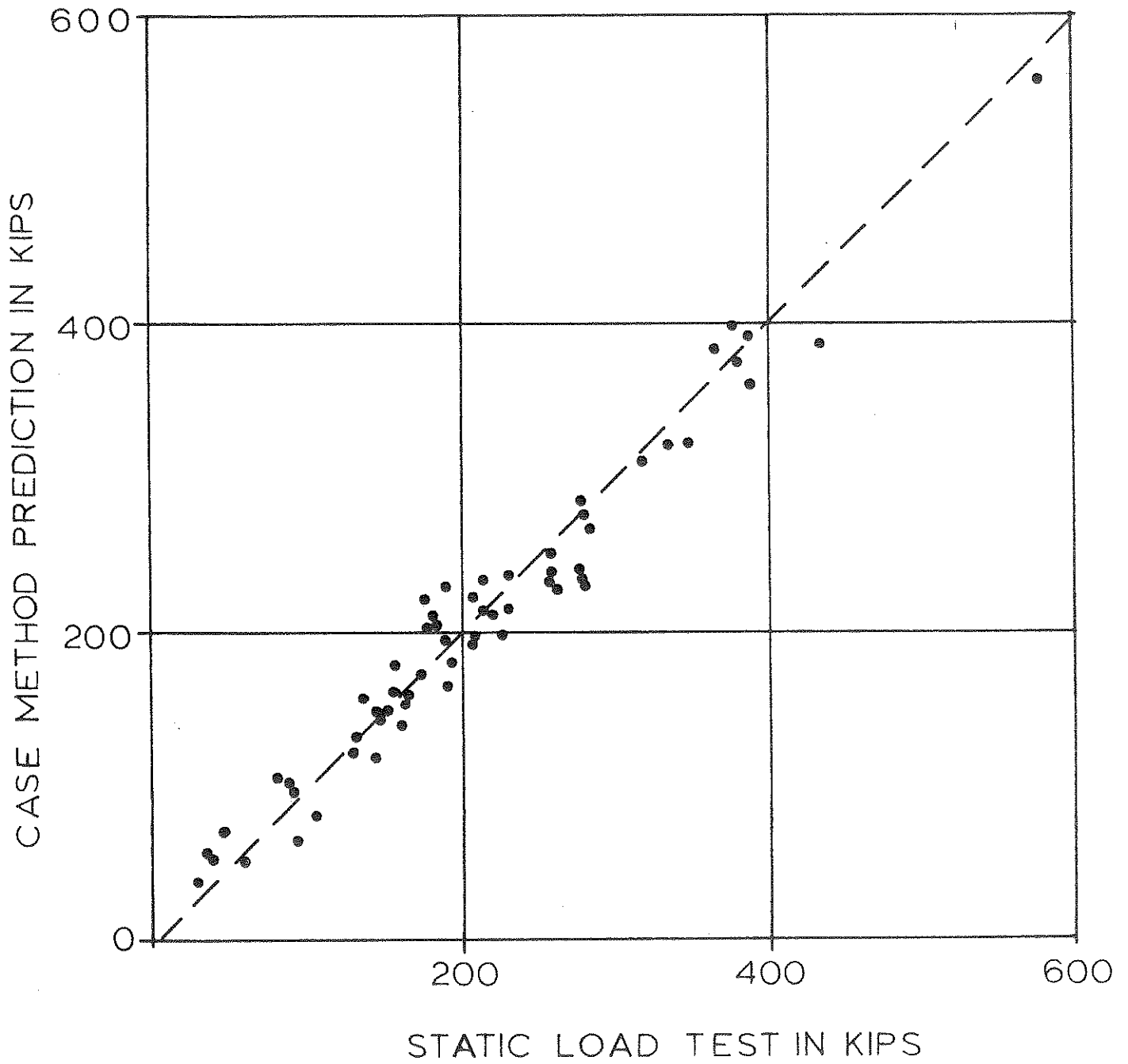


Figure 3.5: Case Method using time delays versus static load test for all pile types

STEEL PIPE PILES

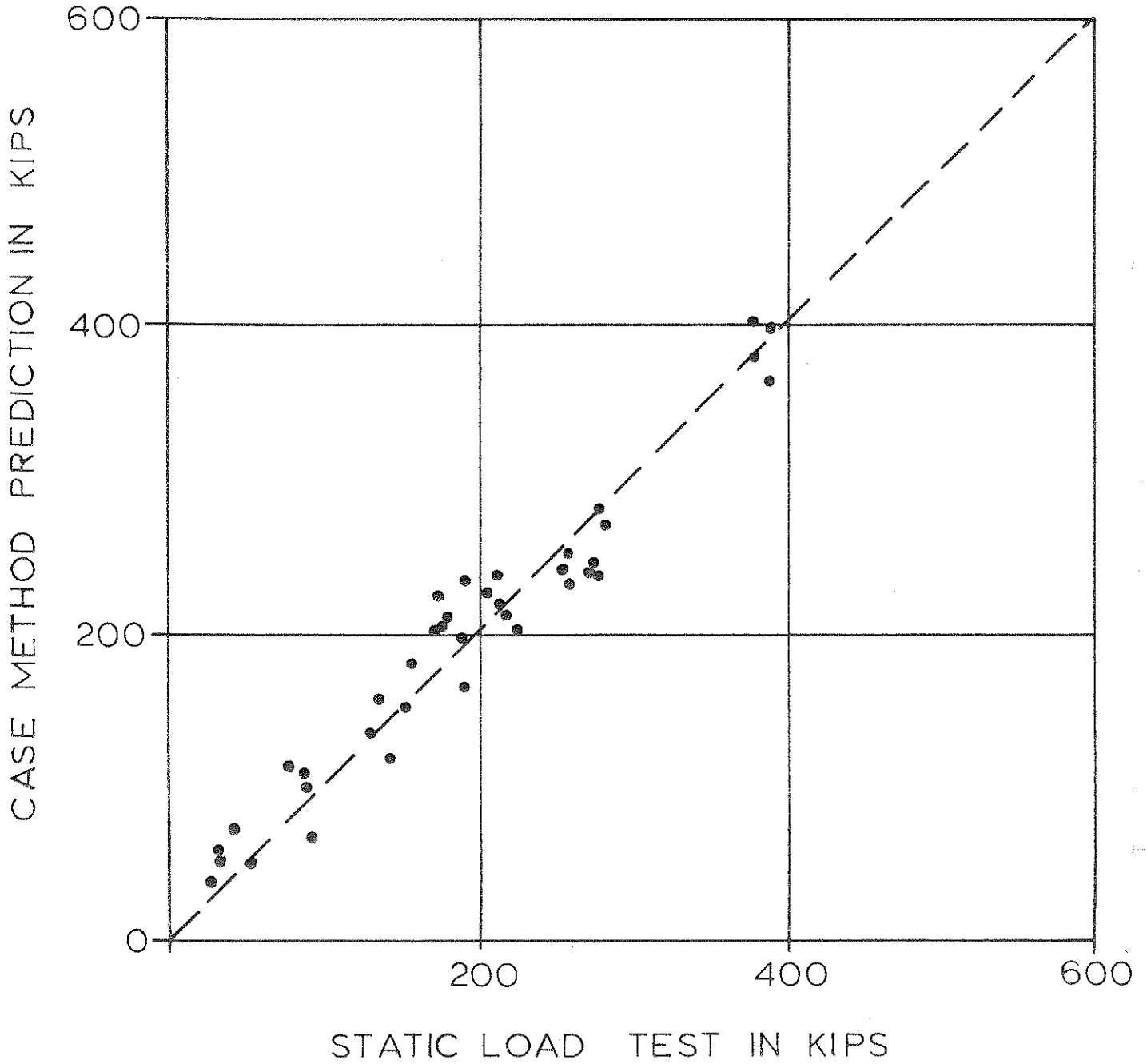


Figure 3.6: Case Method using time delays versus static load test for steel pipe piles.

CONCRETE PILES

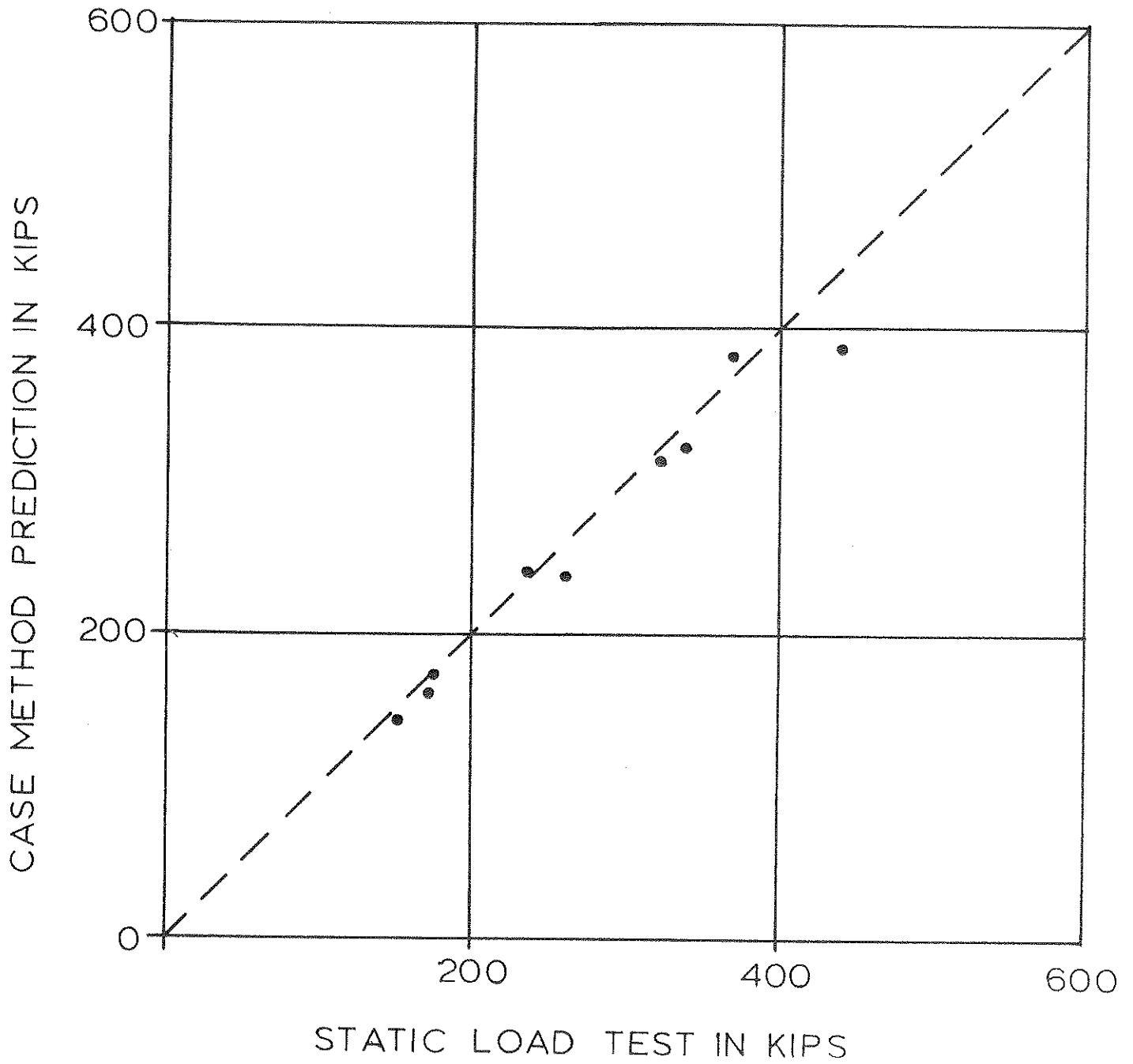


Figure 3.7: Case Method using time delays versus static load test for prestress concrete piles.

TIMBER PILES

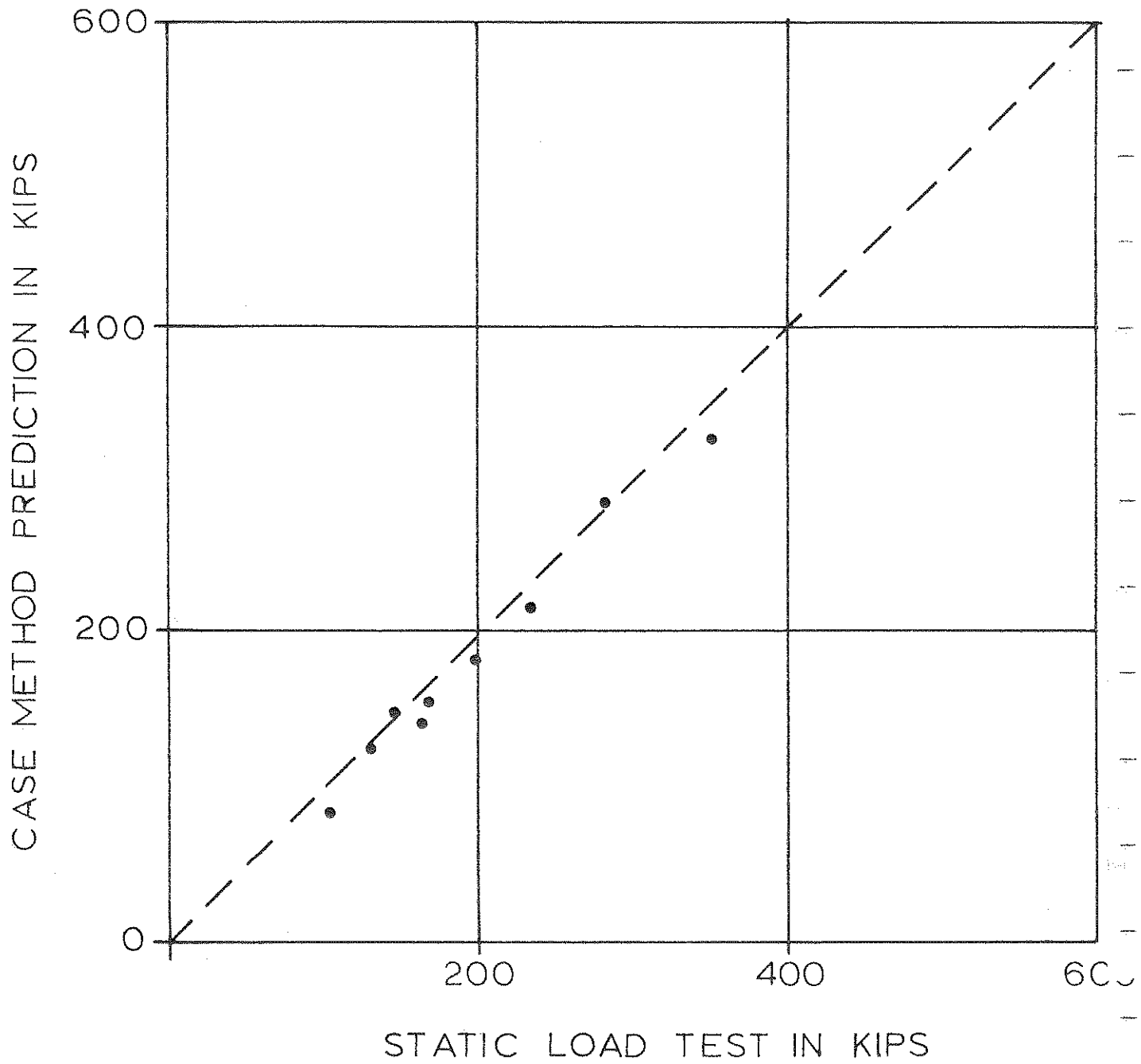


Figure 3.8: Case Method using time delays versus static load test for timber piles.

H PILES

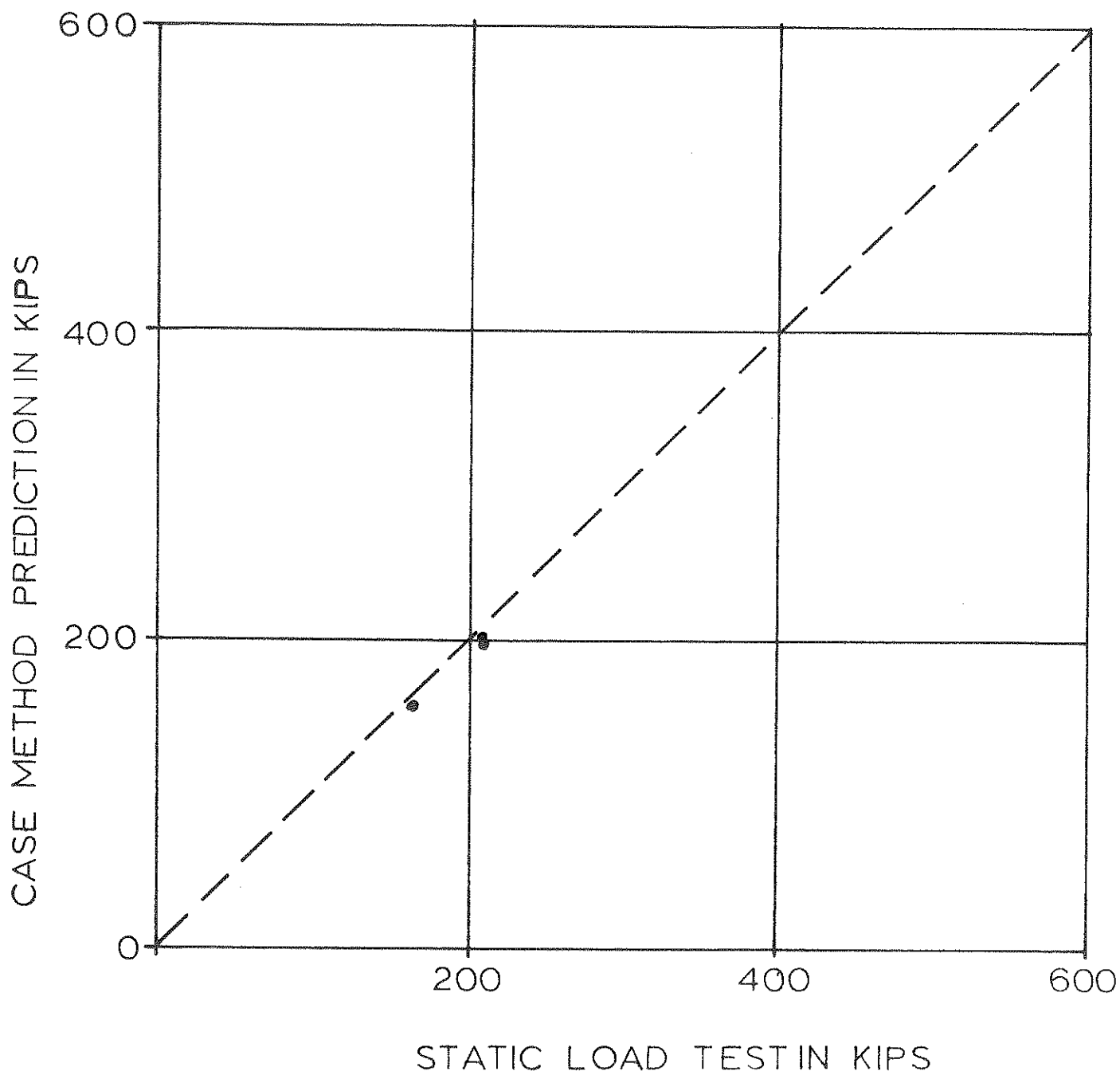


Figure 3.9: Case Method using time delays versus static load test for steel H piles.

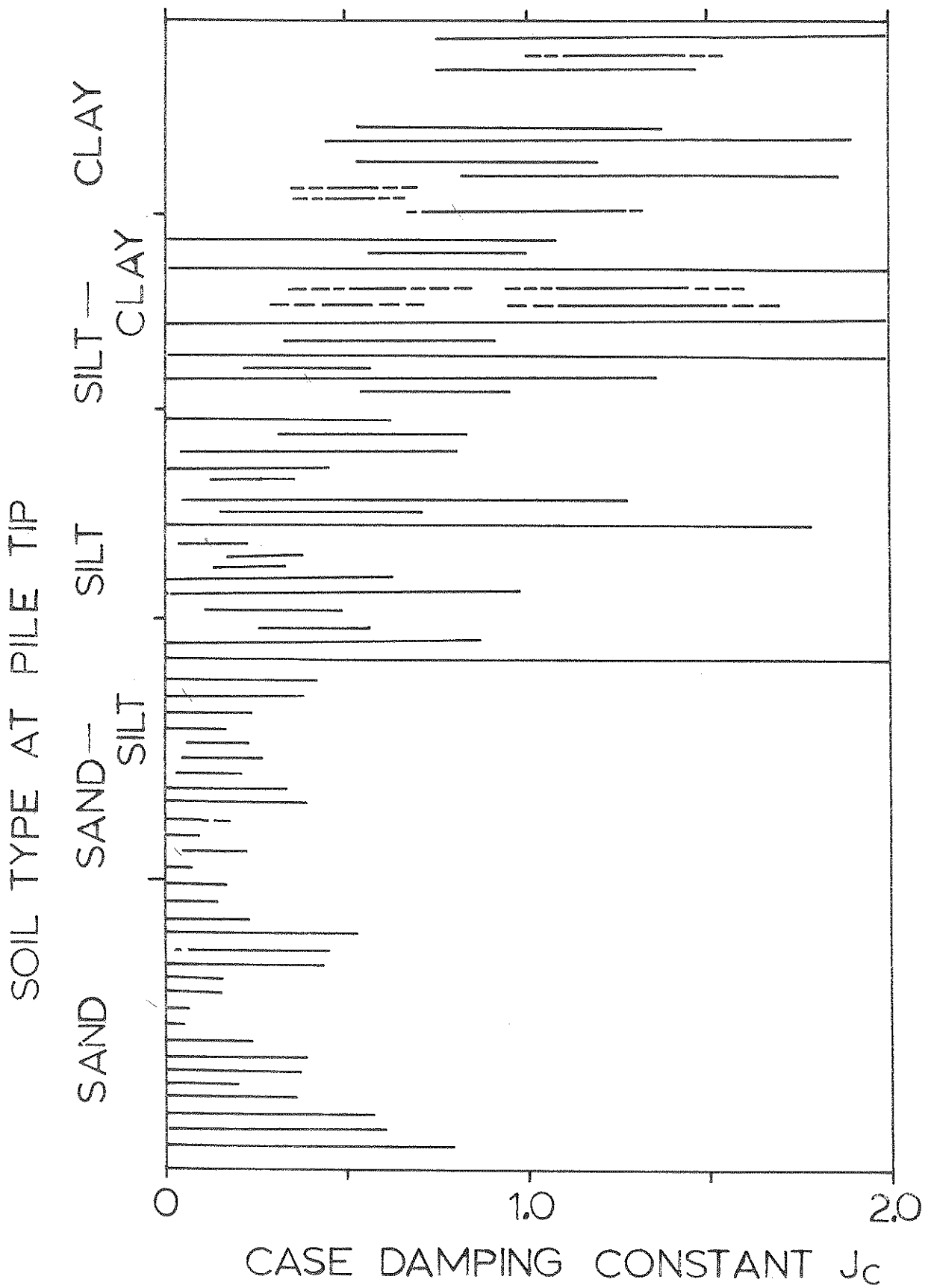


Figure 3.10: Case damping constant J_c giving Case Method prediction within 20% of the static test versus soil type at the pile tip.

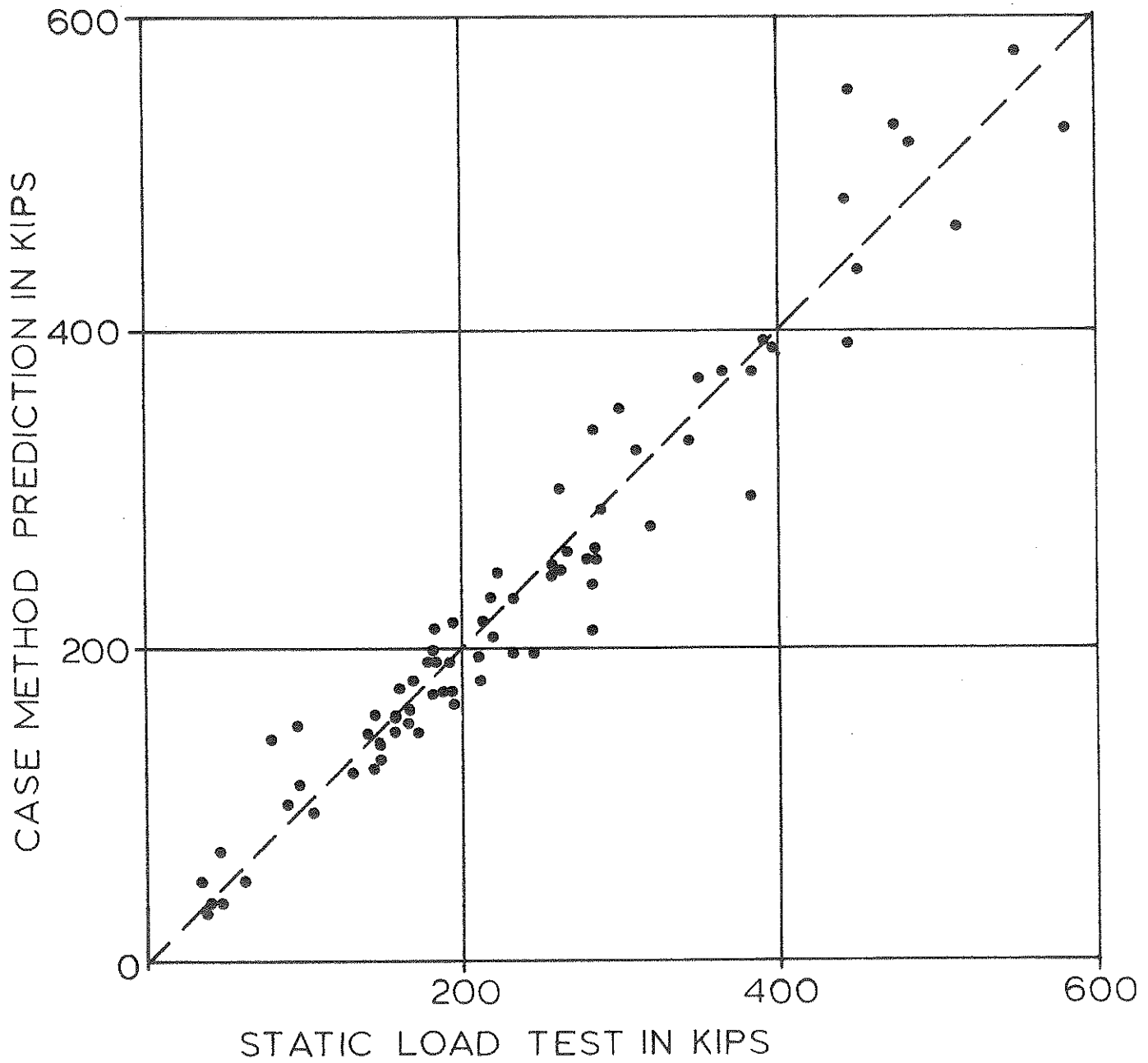


FIGURE 3.11: Case Method Prediction using Case damping technique versus static load test for all pile types

SOIL TYPE AT PILE TIP

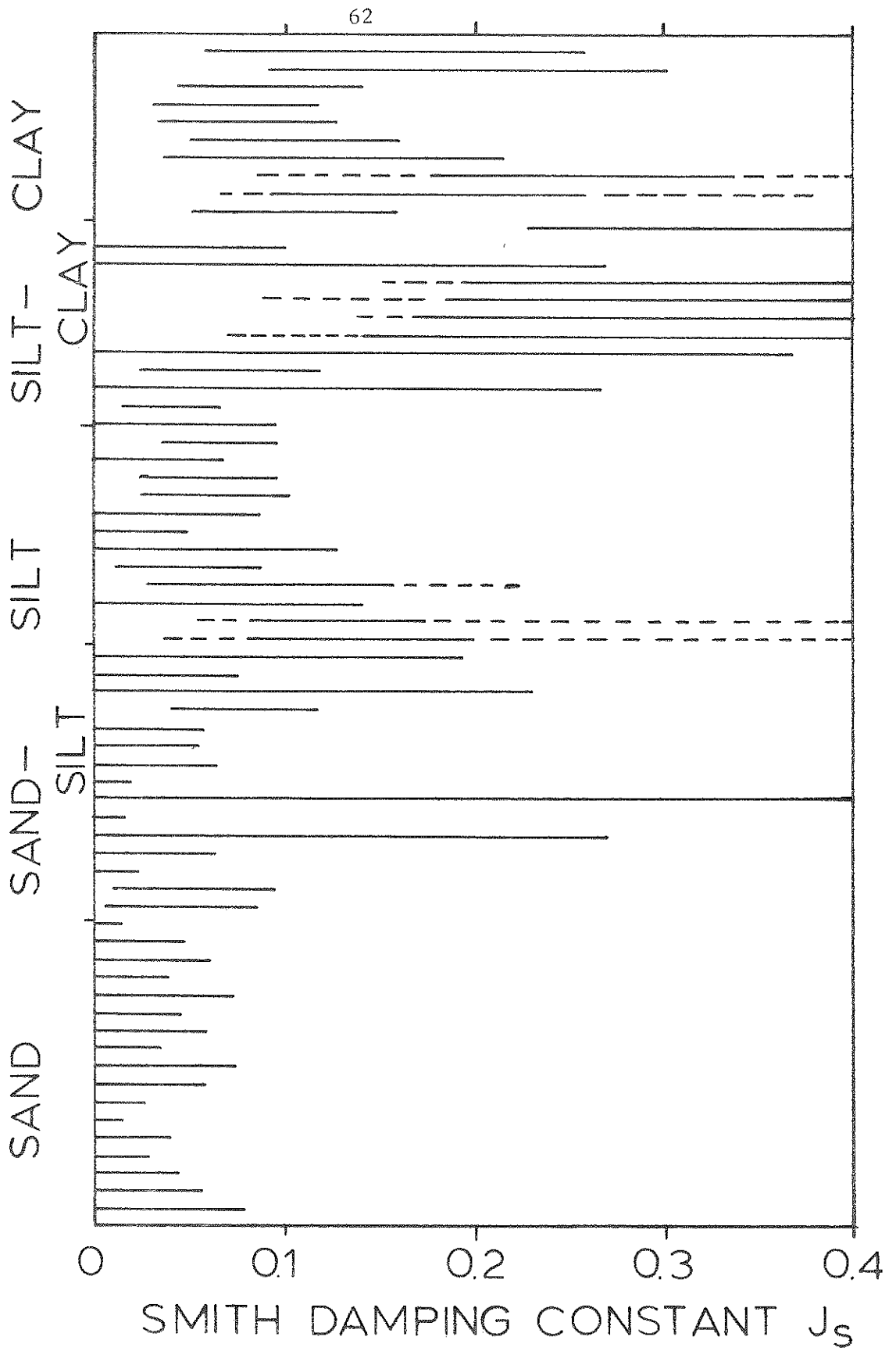


Figure 3.12: Smith damping constant J_c giving Case Method prediction within 20% of the static test result versus soil type at the pile tip.

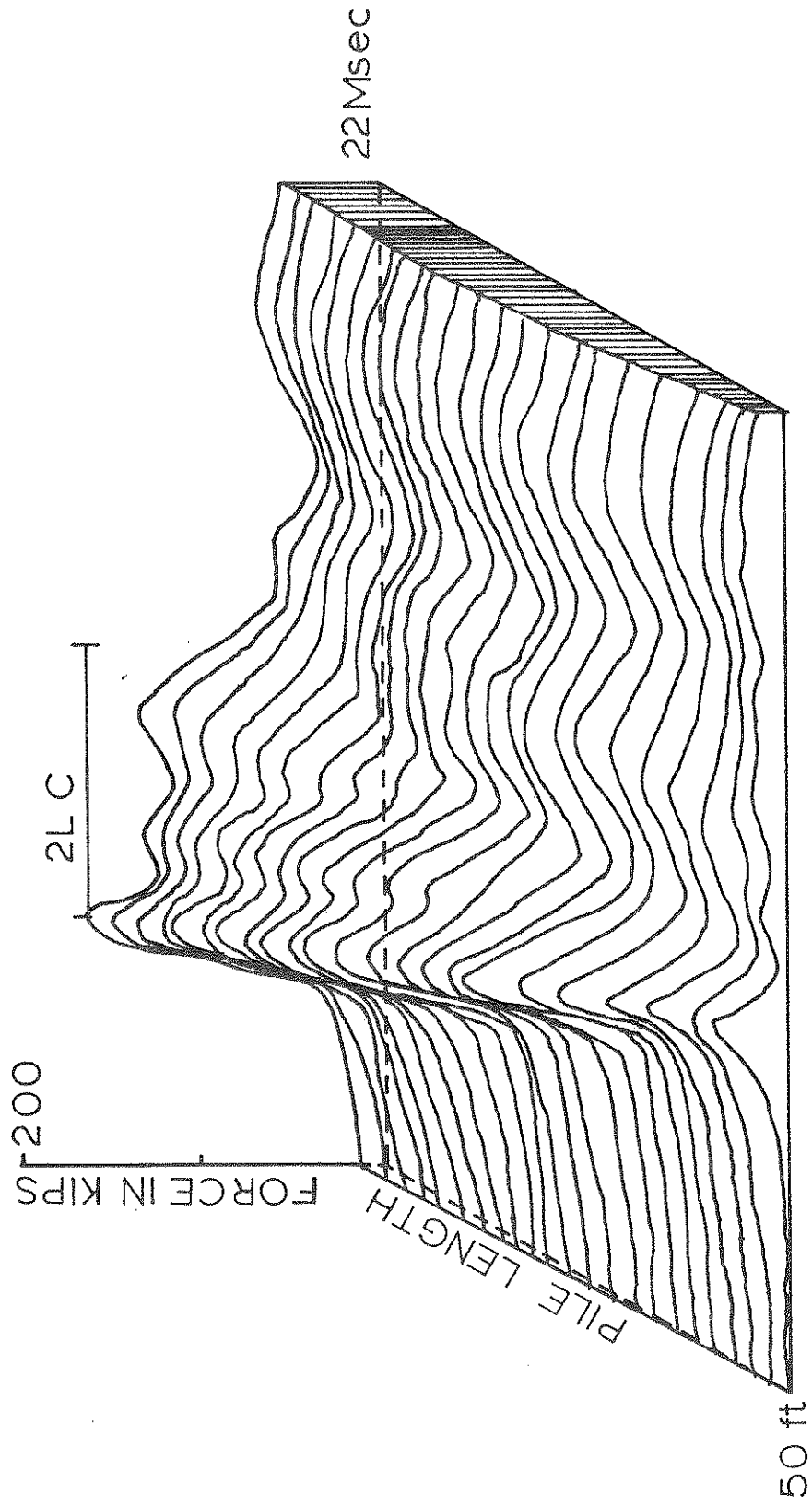


Figure 4.1: Forces in pile versus time for an easy driving condition in Rittman, Ohio.

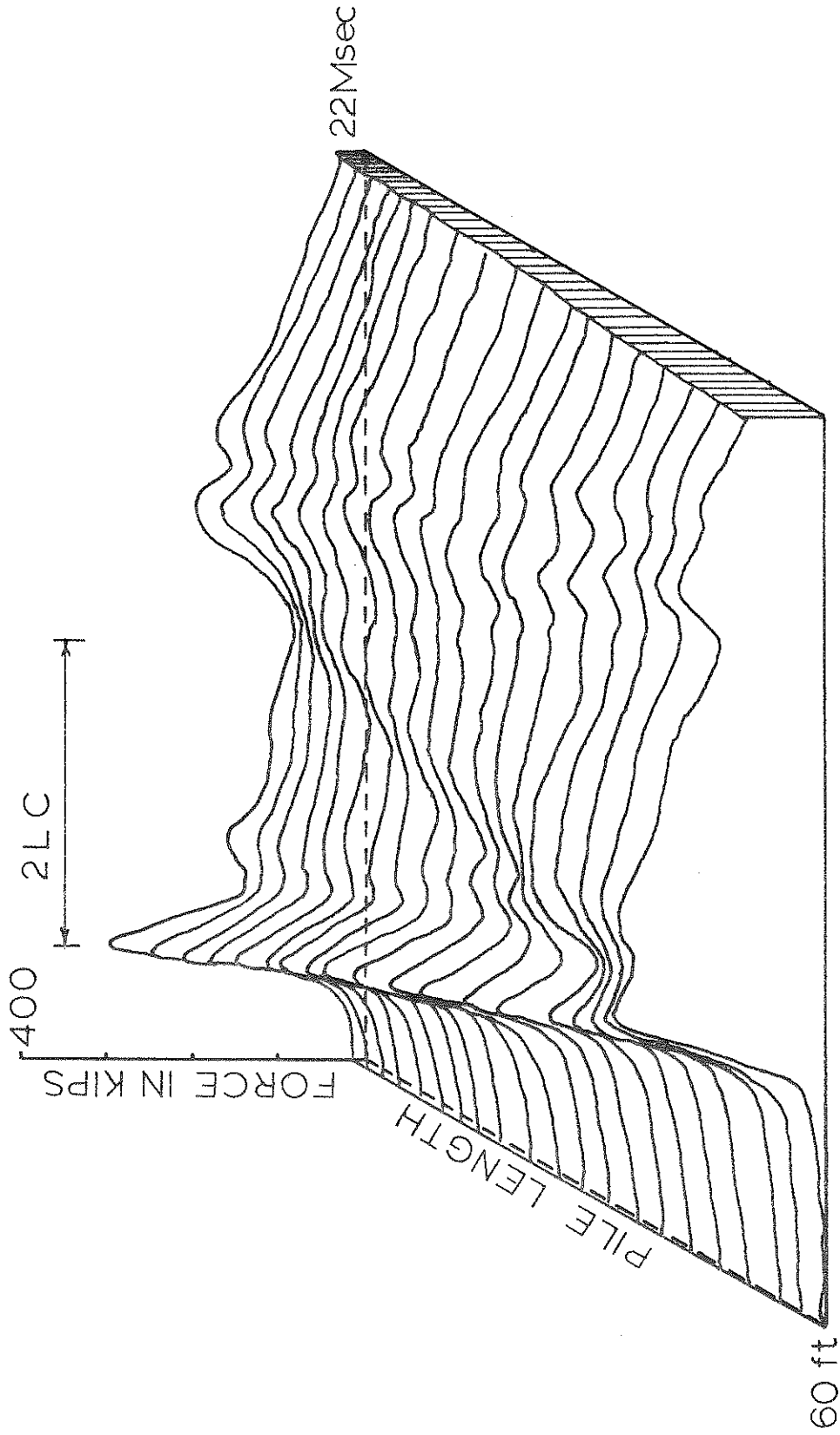


Figure 4.2: Forces in pile versus time for a hard driving condition in Rittman, Ohio.

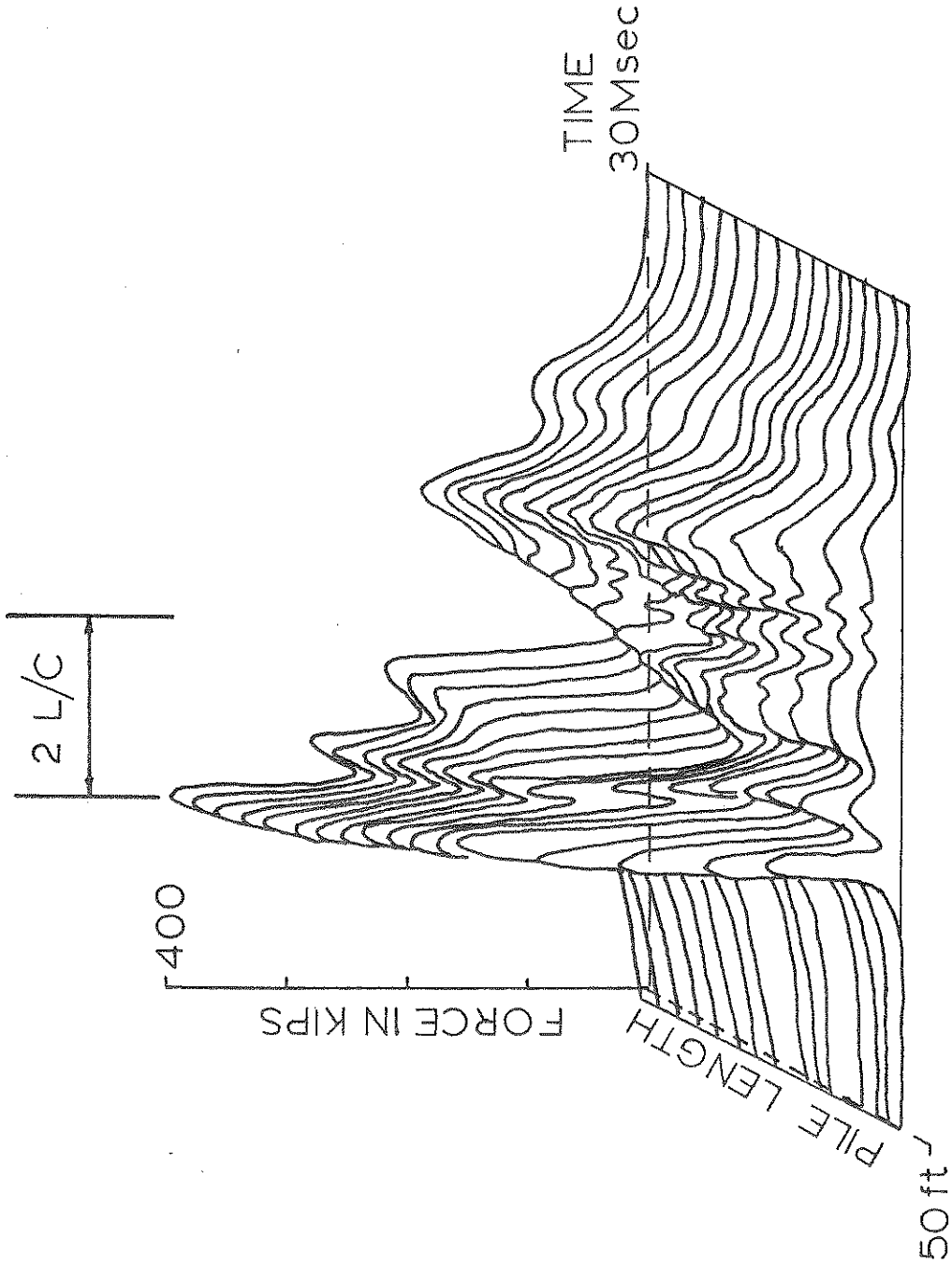


Figure 4.5: Forces in pile versus time for the Purdue test pile in Lafayette, Indiana.

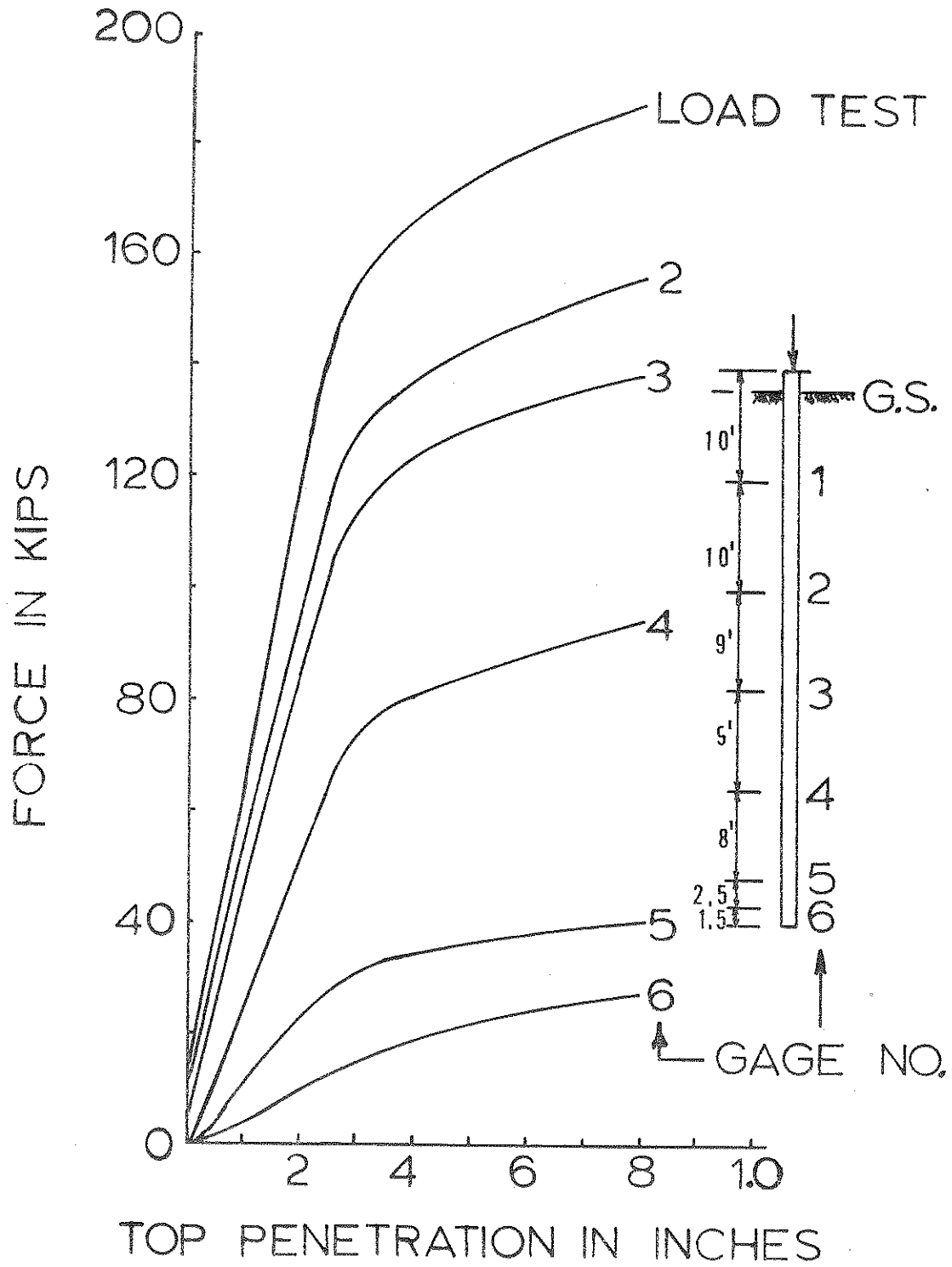


Figure 4.4: Measured forces in pile during Purdue static load test.

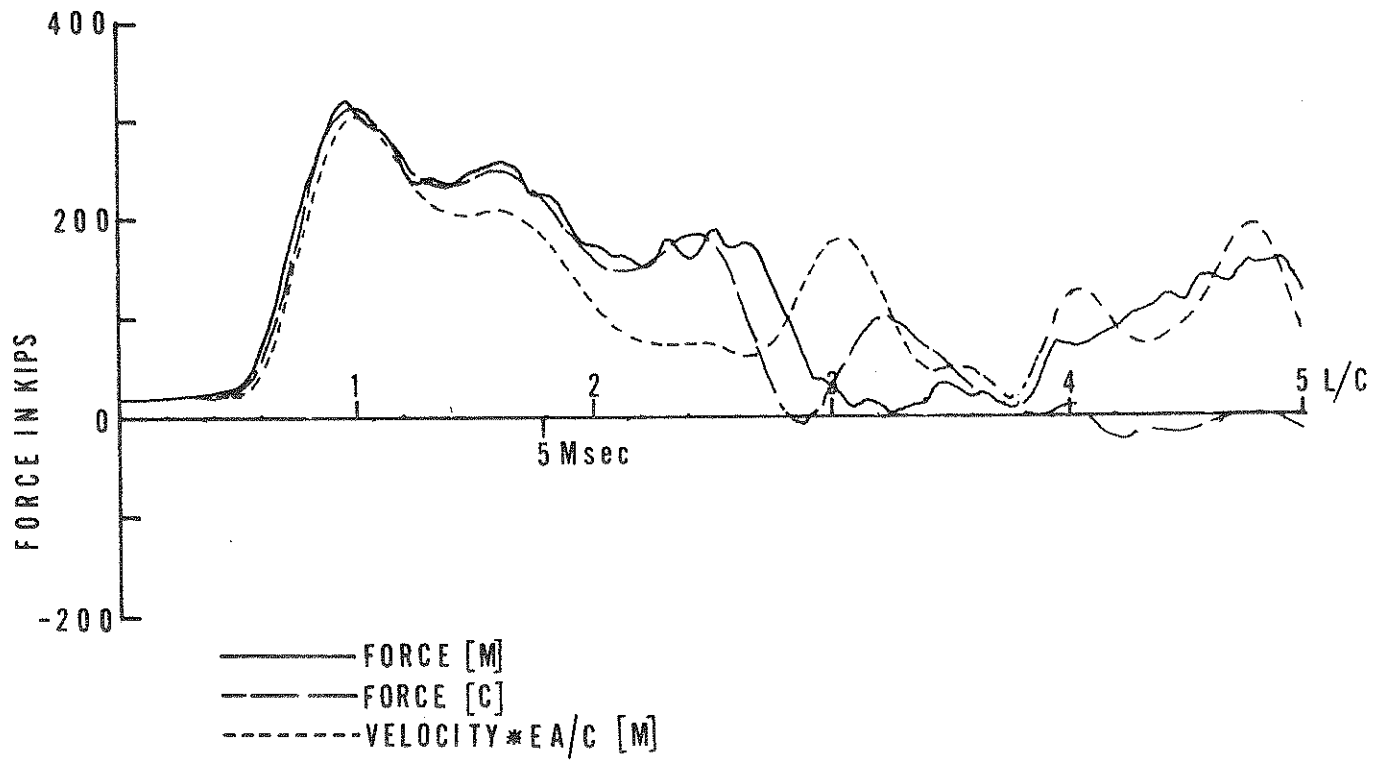
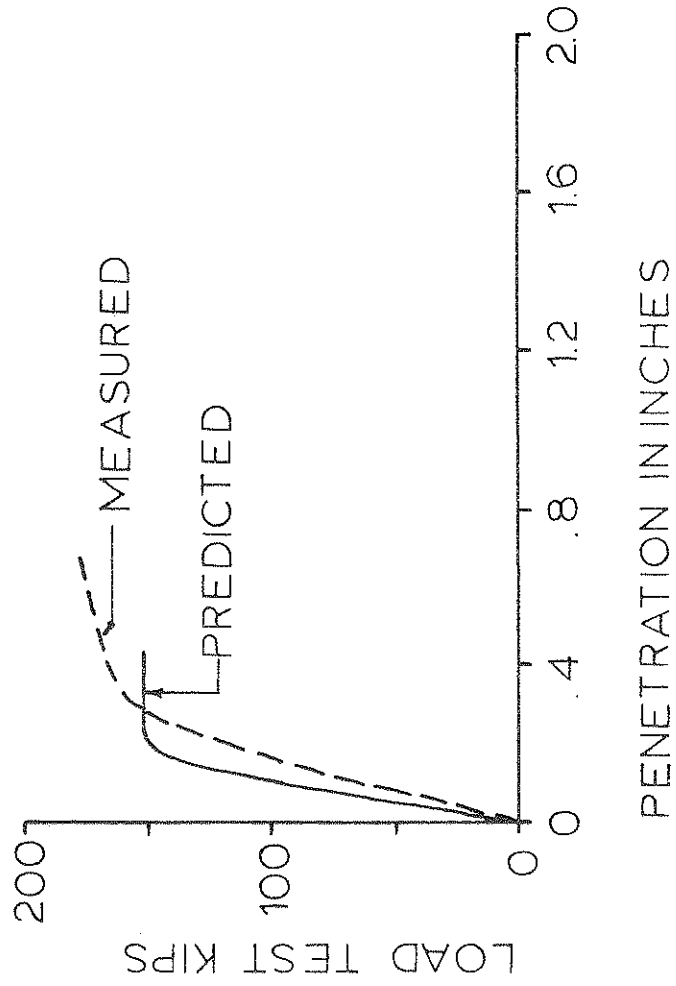
PURDUE LOAD TEST PILE
LAST BLOW

Figure 4.5: Force match computed by CAPWAP for Purdue pile.

PURDUE LOAD TEST PILE
LAST BLOW

A. LOAD TEST CURVES



B. DISTRIBUTION OF
FORCE IN PILE (KIPS)

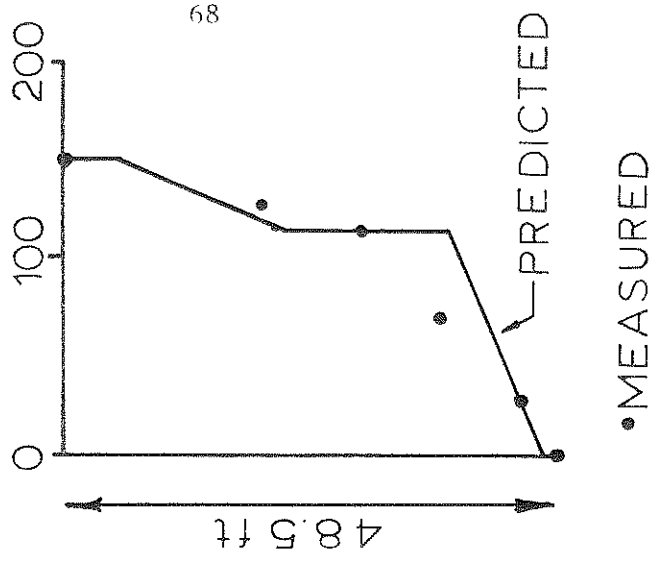


Figure 4.6: CAPWAP predicted and measured static load test curves and force distribution.

ONEONTA, N.Y. LTP
FIRST BLOW

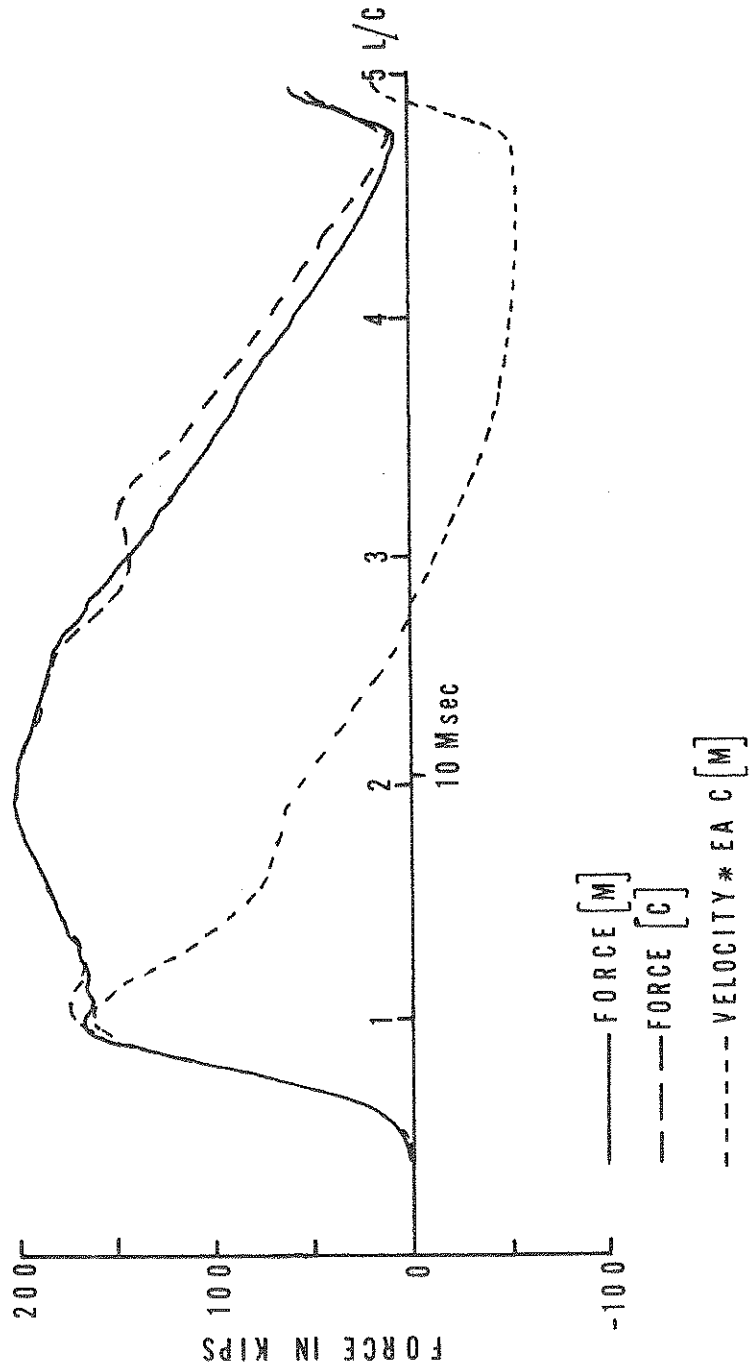
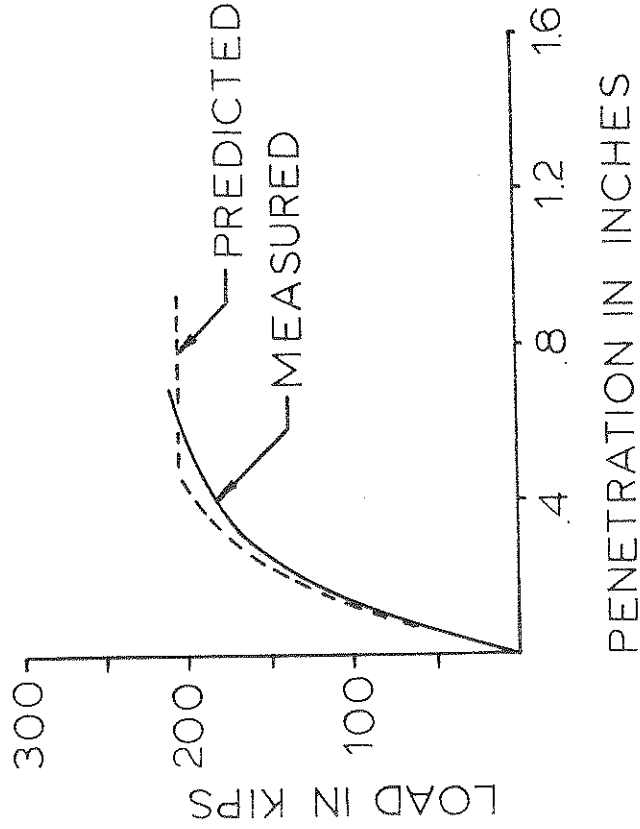


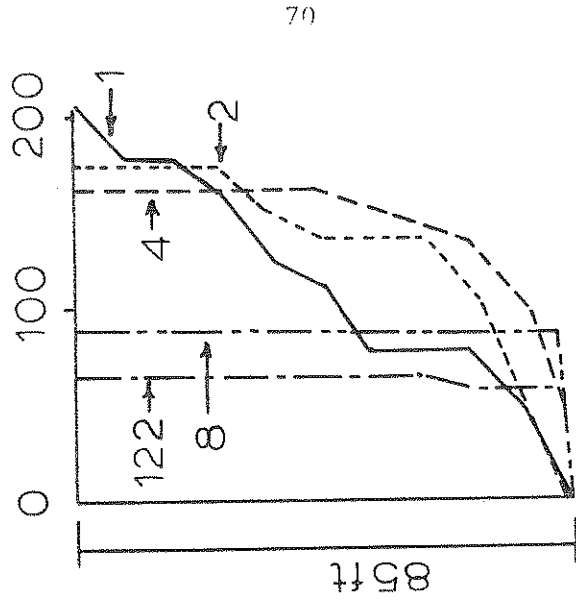
Figure 4.7: Force match computed by CAPWAP for Oneonta test pile.

ONEONTA, N.Y. LTP

A. LOAD TEST CURVES



B. FORCE DISTRIBUTION IN PILE KIPS



PREDICTED (BLOW NO.1)

MEASURED

Figure 4.8: Oneonta load test curves and resistance distribution.

MONTICELLO MINN LTP
EARLY BLOW

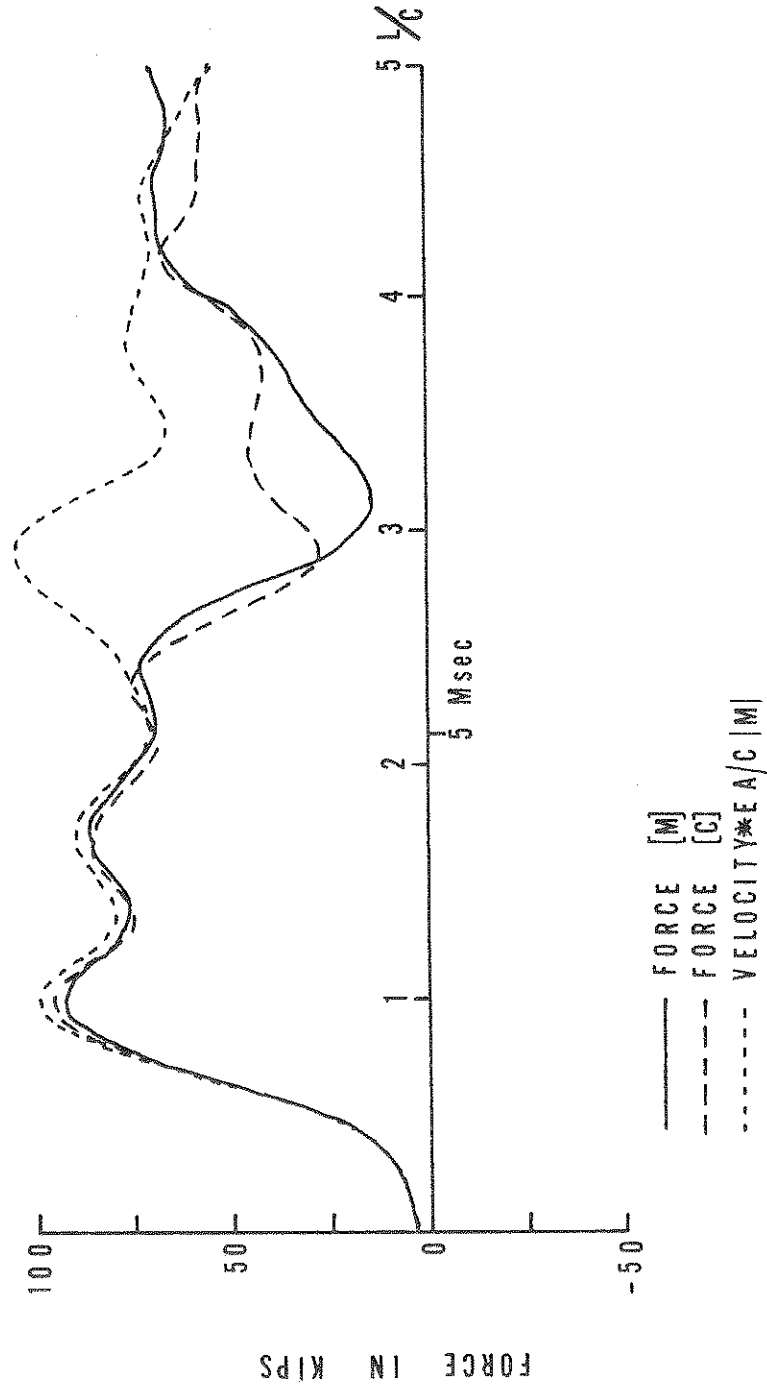


Figure 4.9: Force match computed by CAPWAP for Monticello test pile, early driving.

MONTICELLO MINN LTP
LAST BLOW

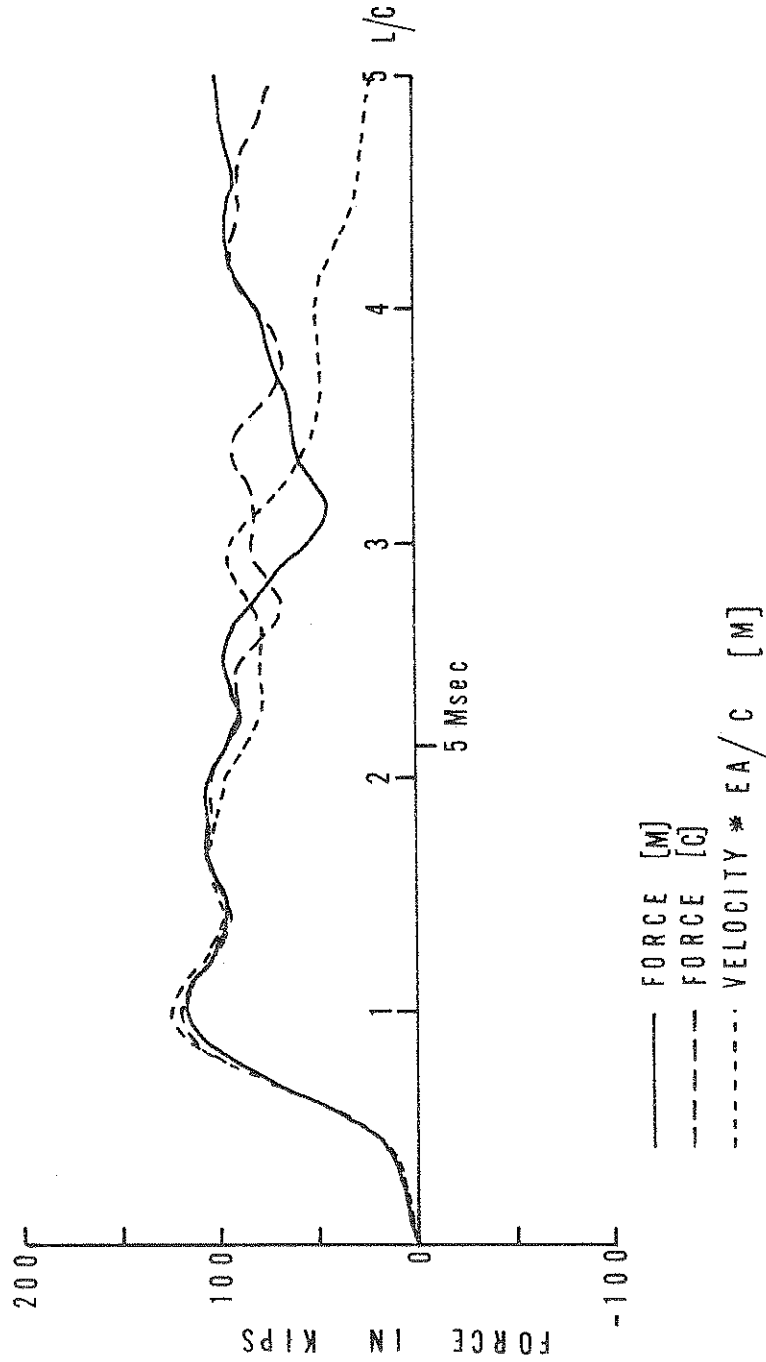
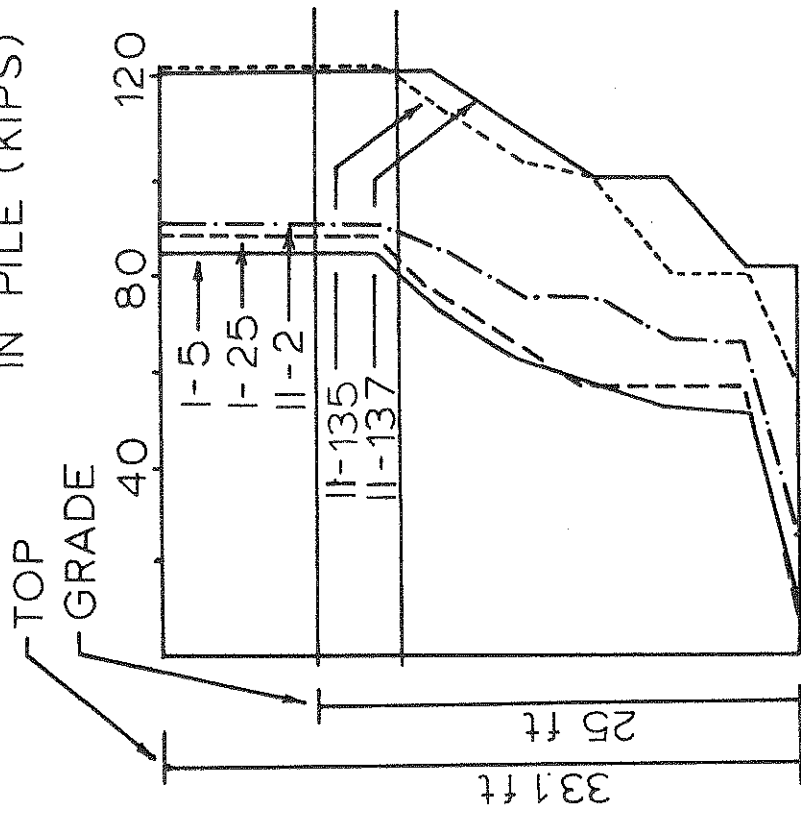


Figure 4.10: Force match computed by CAPWAP for Monticello test pile, last blow of driving.

MONTICELLO MINN. LTP

B. FORCE DISTRIBUTION
IN PILE (KIPS)



A. LOAD TEST CURVES

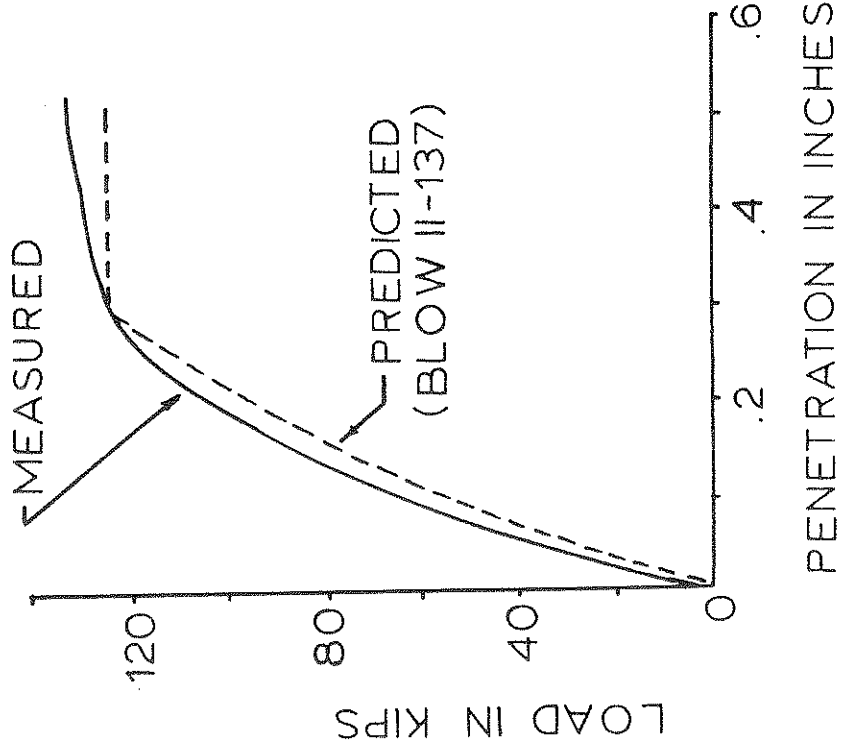


Figure 4.11: Monticello load test curves and resistance distribution.

MIAMI FLA. LTP 2

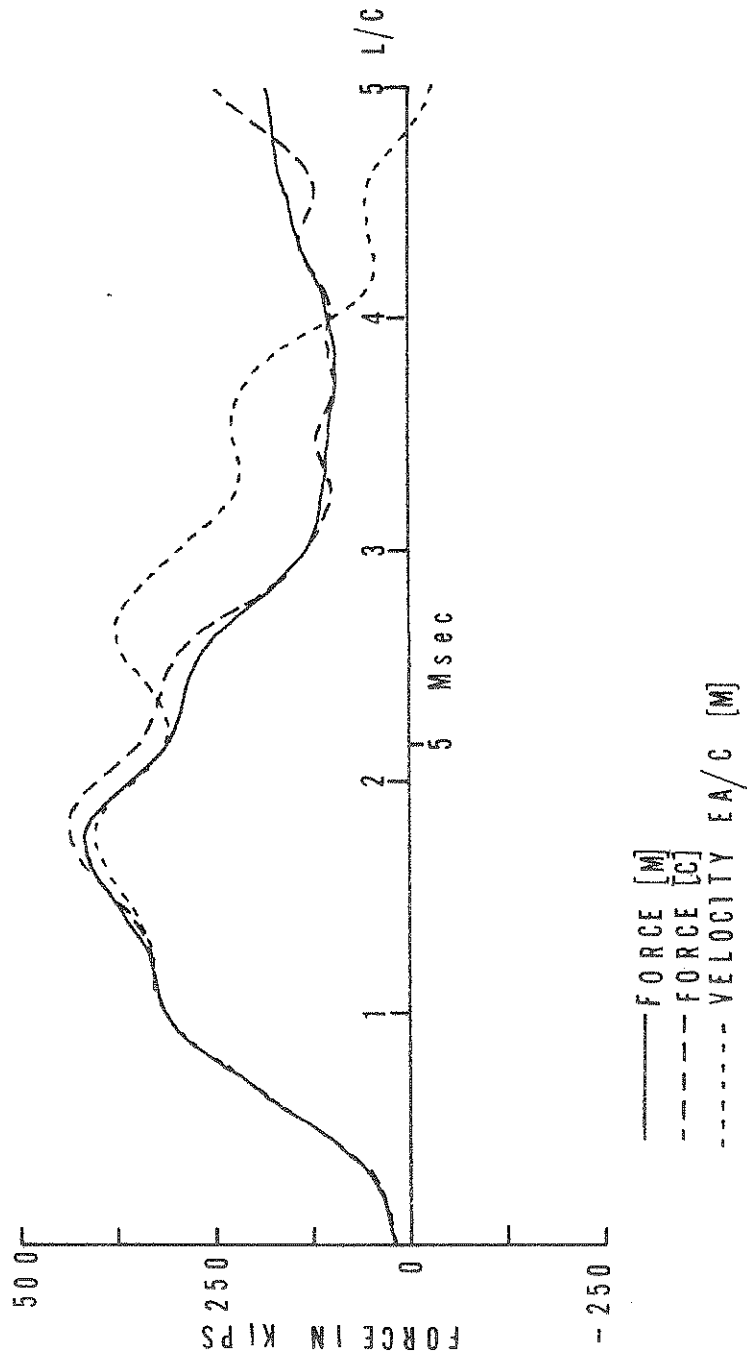


Figure 4.12: Force match computed by CAPWAP for Miami load test pile 2.

MIAMI FLA. LTP 2

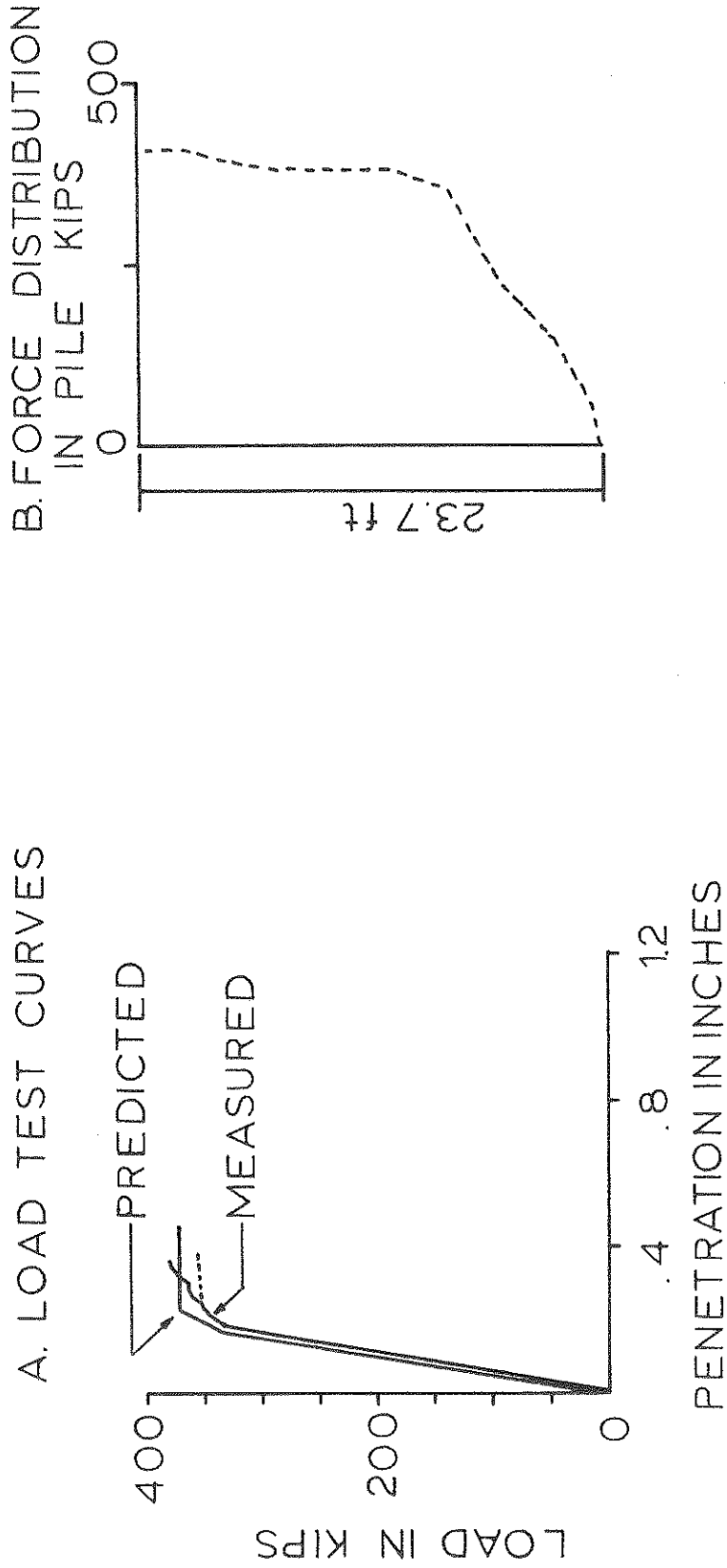


Figure 4.13: Miami load test pile 2 load test curves and resistance distribution.

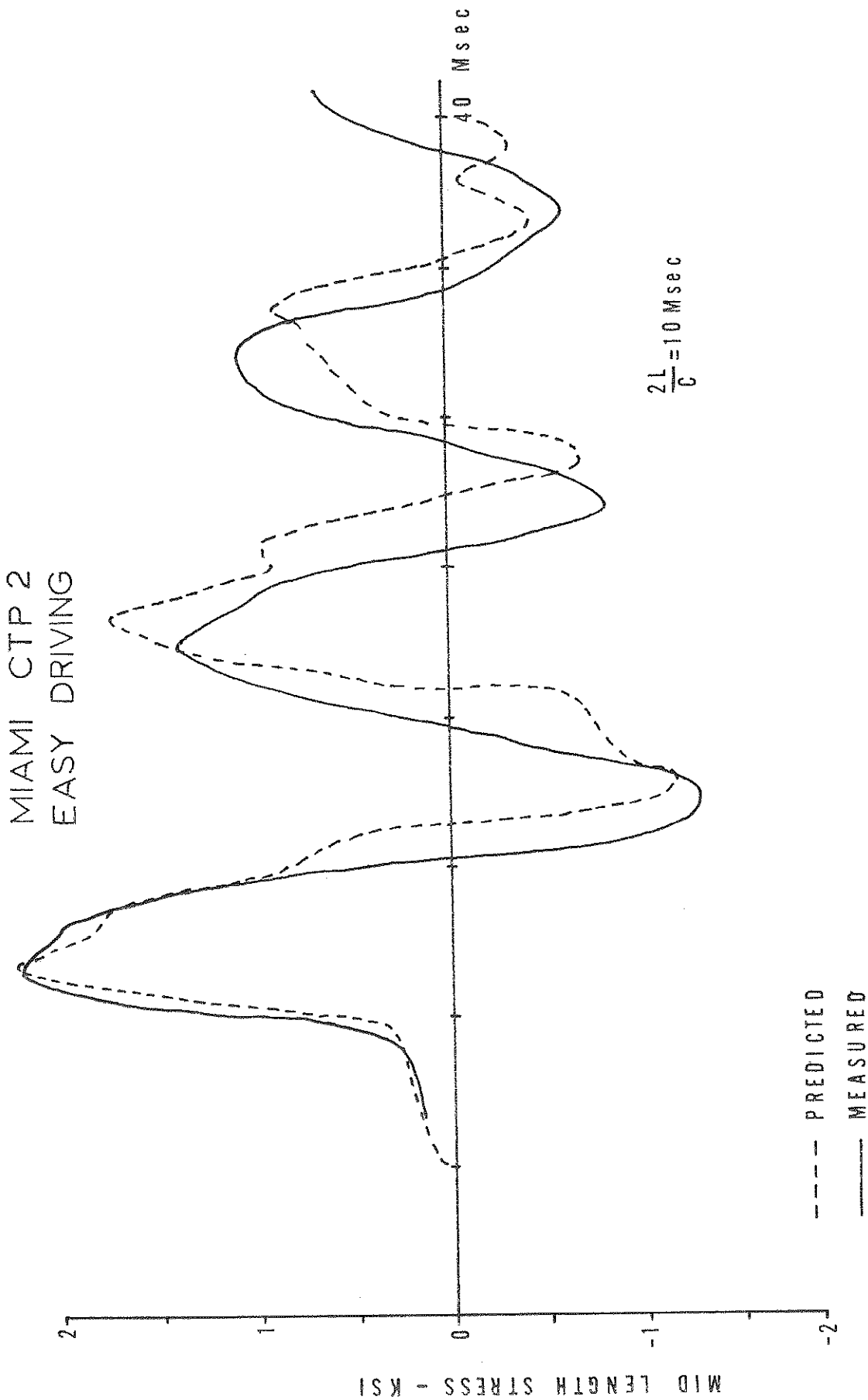


Figure 4.14: Measured and CAPWAP predicted mid length stress during easy driving of a prestress concrete pile in Miami.

MIAMI CTP 2
MEDIUM DRIVING

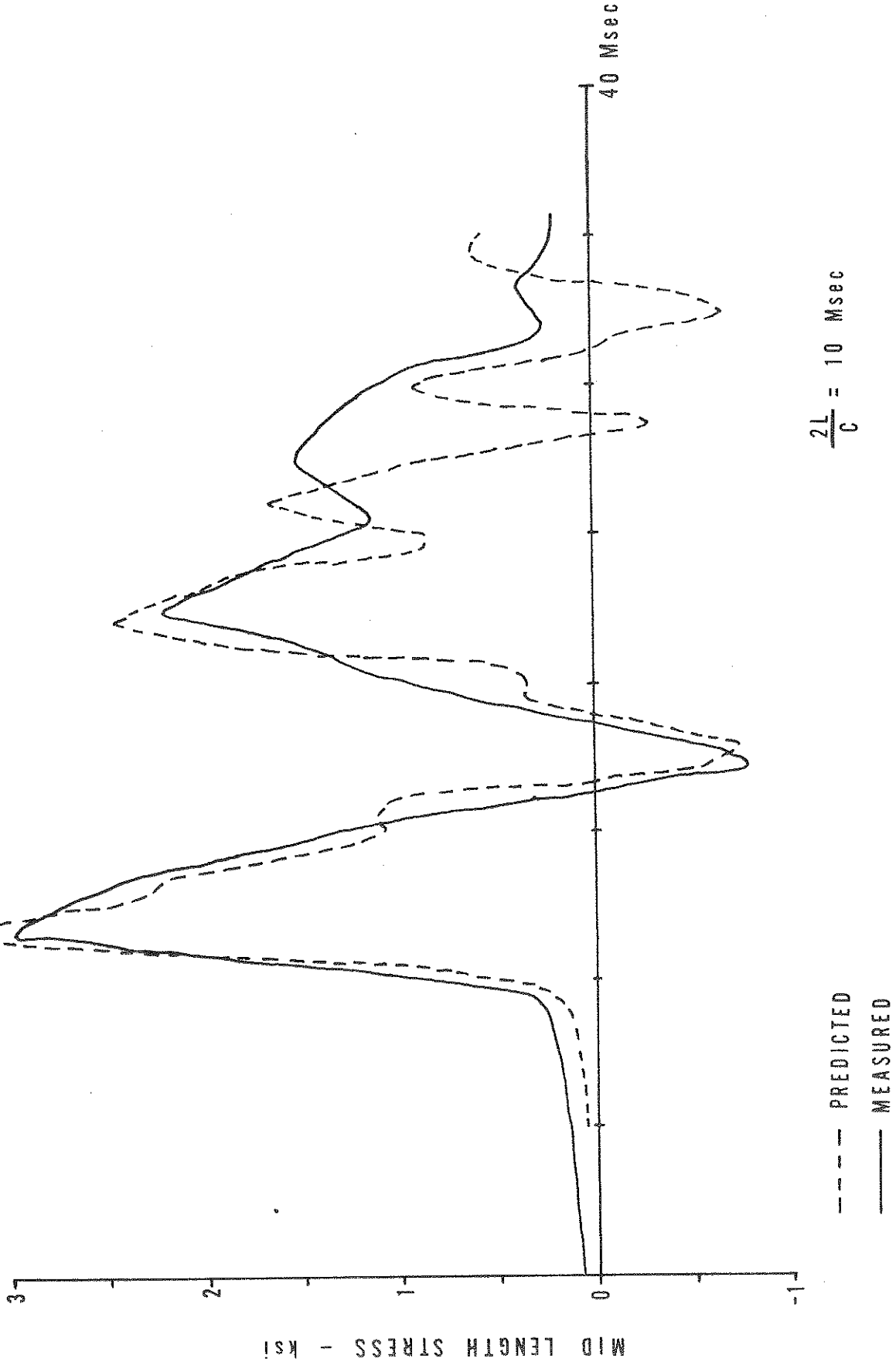


Figure 4.15: Measured and CAPWAP predicted mid length stress during moderate driving of a prestress concrete pile in Miami.